OPTIMIZING GROWTH AND YIELD MODELING IN FORESTRY: LiDAR-DERIVED HEIGHTS FOR LOBLOLLY PINE VOLUME AND WEIGHT ESTIMATION

by

SUVEKSHA JHA

(Under the Direction of Alicia Peduzzi)

ABSTRACT

Forest inventory, an essential component of forestry and natural resource management, heavily relies on the precise measurement of tree height. Nevertheless, the accuracy of this measurement is often compromised by instrumental inaccuracies and human subjectivity. To address these challenges, this thesis explores the potential of Light Detection and Ranging (LiDAR) technology as an alternative solution, offering a reduction in instrument-related errors and the elimination of human biases. In the initial chapter, we investigate the pivotal role of tree height in developing growth and yield models. Through comprehensive analysis and comparisons between various LiDAR data height extraction methods and field inventory height measurements, we establish that LiDAR-derived heights, specifically from 'pixel_metrics,' closely align with field data. We leverage these findings to incorporate LiDAR-derived height projections into yield prediction equations, unveiling LiDAR's superior performance over traditional field measurements in several metrics. When contrasting projected field volume with actual volume in the second year, LiDAR-estimated volume (Adj. $R^2 = 0.85$) exhibits a slight advantage over field projections (Adj. $R^2 = 0.85$). Similarly, in green weight calculations, LiDAR-predicted green weight in year 2 (Adj. $R^2 = 0.85$) slightly outperforms field-derived green weight (Adj. $R^2 = 0.84$).

In the third chapter, our exploration expands to encompass Unmanned Aerial Vehicle (UAV) derived LiDAR data characterized by high point density. This expansion introduces enhanced resolution and examines its correlation with forest volume and green weight using PMRC 2014 equations. Our LiDAR metrics model for volume gives an R-squared (Adj. R^2) value of 0.79, while the green weight model exhibits an Adj. R^2 value of 0.81. Although this approach shows immense potential, we also observe minor discrepancies in volume and biomass estimates, which can be attributed to factors such as the lack of data for lower yield values and variations in data variability between LiDAR and PMRC estimates. Nonetheless, this study highlights the potential of UAV LiDAR data as a valuable tool for precise forest inventory at the plot level. The innovative methods explored in this thesis, combined with data analysis, hold the potential to transform forest management, providing more accurate assessments and contributing to the sustainability of natural resource management.

INDEX WORDS: forest inventory, dominant height, volume, weight, *Pinus taeda*, southern pine, human bias, forest management, growth and yield model

OPTIMIZING GROWTH AND YIELD MODELING IN FORESTRY: LIDAR-DERIVED HEIGHTS FOR LOBLOLLY PINE VOLUME AND WEIGHT ESTIMATION

by

SUVEKSHA JHA

B.Sc., Tribhuvan University, Nepal, 2021

A Thesis Submitted to the Graduate Faculty of The University of Georgia in Partial Fulfillment of the Requirements for the Degree

MASTER OF SCIENCE

ATHENS, GEORGIA

2023

OPTIMIZING GROWTH AND YIELD MODELING IN FORESTRY: LIDAR-DERIVED HEIGHTS FOR LOBLOLLY PINE VOLUME AND WEIGHT ESTIMATION

by

SUVEKSHA JHA

Major Professor:	Alicia Peduzzi
Committee:	Cristián R. Montes
	Deepak Mishra

Electronic Version Approved:

Ron Walcott
Vice Provost for Graduate Education and Dean of the Graduate School
The University of Georgia
December 2023

ACKNOWLEDGEMENTS

First and foremost, I would like to acknowledge my graduate advisor, Dr. Alicia Peduzzi. Her guidance and support throughout this degree were essential in accomplishing my master's. Her personal connection, mentorship, understanding, and kindness have been a constant source of inspiration for me as I move forward in my academic journey.

I extend my sincere gratitude to the committee members, Drs. Cristian Montes, and Deepak Mishra, for generously allocating their valuable time to attend meetings, review my work, and provide insightful suggestions that significantly improved the quality of my research.

My deep appreciation goes to the Warnell School of Forestry and Natural Resources at the University of Georgia, the Plantation Management Research Cooperative (PMRC), and the Precision Forestry Lab for their generous funding and unwavering support, which were instrumental in helping me complete my degree. I am eternally grateful to the researchers, staff, field crew, and cooperative members of the PMRC, as well as the skilled drone pilot and research professional, Jackson Glomb, for providing the necessary resources, data, and opportunities that facilitated the successful completion of my research.

This achievement would not have been possible without the constant love and support of my family and friends. Their support and patience have been an invaluable source of strength. I am also appreciative of my fellow graduate students in the Precision Forestry Lab and PMRC lab, who not only provided help and ideas but also made this program more enjoyable throughout these years.

TABLE OF CONTENTS

LIST OF FIGURES

LIST OF TABLES

INTRODUCTION

Across the southern United States, vast expanses of forestland, stretching over 10 million hectares of naturally regenerated pine forests, and an additional 14 million hectares dedicated to pine plantations, play a pivotal role in shaping the environment, society, and economy(Jeffrey P. Prestemon, 2002). Over the past half-century, these forests have experienced a remarkable transformation, with their productivity increasing three times (Jokela, Martin, & Vogel, 2010). Among commercially important species, Loblolly pine (*Pinus taeda*) is known as the most extensively planted and has been increasing in demand. This remarkable surge in productivity is attributed to a range of silvicultural techniques, including careful site preparation, the control of competing vegetation, soil enrichment through fertilization, and the use of genetically enhanced seedlings (Borders et al., 2014; Zhao et al., 2019). Understanding the dynamics of pine growth within these forests is essential for effective silvicultural management, enabling forest managers to make informed decisions regarding growth and yield projection.

Growth and yield modeling forms the basis of managing these pine plantations effectively. Existing models for loblolly pine productivity depend on factors like tree species, age, density, size, and site quality (Avery & Burkhart, 1983). Of these factors, tree size is crucial, and it is typically assessed through measurements of diameter and height (Schumacher & Hall, 1933). Traditional methods of height measurement, however, are prone to errors stemming from instrumentation and operator subjectivity (Yang & Burkhart, 2020). To address this challenge, LiDAR (Light Detection and Ranging) technology offers a convincing solution. LiDAR has the potential to reduce sampling requirements, and its accuracy surpasses that of traditional inventory

techniques (Matti Maltamo, 2014; Naesset, 1997). Despite these advantages, determining the optimal method for extracting tree heights from LiDAR data remains an open question, with both raster and echo metrics-based methods under consideration. Furthermore, the role of LiDAR-derived heights in long-term volume and weight projection models has received limited attention. In this study we will use the best optimal LiDAR derived height and project it using PMRC 1996 projection model (Harrison & Borders, 1996) to see how insignificant they are with traditionally measure tree heights. Also, the comparison of how LiDAR projected height would be in yield equations of PMRC will be done.

Numerous previous studies have explored the application of LiDAR variables in predicting yield, encompassing volume and biomass estimation (Bortolot & Wynne, 2005; Cao et al., 2016; Chris Hopkinson, 2008; Popescu, 2007; Silva et al., 2017c). The majority of existing studies have only investigated the yield in a single time. Consequently, the utilization of multi-temporal LiDAR data holds the promise of broadening the horizons of LiDAR remote sensing, expanding its potential for applications in volume, weight, and diverse projection modeling (Hudak, Evans, & Stuart Smith, 2009). This potential shift is especially significant given that, until now, growth quantification in plantations has primarily relied on airborne laser scanning, with a predominant emphasis on simple change detection in cases where multi-temporal LiDAR data were accessible. Considering recent advancements, we recognize the enormous promise inherent in LiDAR technology, especially when combined with enhanced point density and Unmanned Aerial Vehicles (UAVs). This amalgamation not only facilitates projection and measurement but also ensures the precise quantification of the total yield within pine plantations. This research lies utilizes three distinct datasets, encompassing actual field data acquired through conventional forest

inventory techniques and three sets of LiDAR data. The result of this study will provide forest managers with indispensable tools, empowering them to make forecasts based on objective and thoroughly used forest modeling resources.

SITE DESCRIPTION

This research was conducted within seven distinct loblolly pine installations, encompassing four sites falling under the Coastal Plain Culture Density (CPCD) study area and three sites belonging to the South Atlantic Gulf Slope Studies (SAGSCD). All these installations are meticulously managed by the University of Georgia Plantation Management Research Cooperative (PMRC). Specifically, the SAGSCD installations are situated in Alabama, while the CPCD installations are geographically dispersed, spanning across the states of Georgia, South Carolina, and Florida. These installations were particularly selected due to the availability of previously acquired USGS LiDAR data. The PMRC initiated the CPCD study during the 1995/96 period, while the SAGSCD study commenced in 1997/1998. These two extensive studies share a common set of overarching objectives:

Quantify and Contrast Growth and Yield Effects: The primary aim is to meticulously assess and differentiate the impacts of intensive silviculture and current operational practices on the growth and yield of loblolly and slash pine plantations. These evaluations encompass a broad spectrum of densities.

Explore Cultural Intensity and Density Interactions: A key facet of the research involves investigating potential interactions between cultural intensity and stand density. This investigation extends to various aspects, including survival rates, merchantable green and dry weight production, and the distribution of product classes.

The study sites were subjected to two distinct levels of management intensity, each with a well-defined set of treatments. In summary, the operational treatment involved specific steps to promote pine tree growth:

Spring Bedding and Herbicide Treatment: Spring bedding was conducted, followed by a fall herbicide application. The herbicide formulation depended on the type of competition: 12 oz. Arsenal plus 1 qt. Garlon 4 per acre for waxy-leafed species, or 12 oz. Arsenal plus 1 qt. Accord per acre for grass and upland hardwood competitors. Herbicide was applied in a 5-foot band over the rows. Additionally, 500 lbs. of 10-10-10 fertilizer were applied at planting.

The intensive cultural treatment consisted of:

Spring Bedding and Herbicide Application: Similar to the operational treatment, spring bedding was followed by a fall herbicide application. The herbicide treatment comprised 16 oz. Arsenal, 2 qts. Garlon 4, and 2 qts. Accord per acre. Again, 500 was of 10-10-10 fertilizer was applied at planting.

Nutrient Enhancement: In the third growing season, 600 lbs/ac 10-10-10 fertilizer, along with micronutrients, and 117 lbs/ac NH_4NO_3 were applied. An additional 117 lbs/ac NH_4NO_3 were added in the fourth growing season.

Vegetation Control: Starting in the first growing season (1996), plots were treated with 4 oz. Oust per acre, and directed sprays were used to eliminate competing vegetation.

Insect Control: Insecticides, usually Pounce, were applied as needed to manage tip moths during the initial two growing seasons.

Within both treatment types, six loblolly pine subplots with varying tree densities ranging from 300 to 1800 trees per acre (tpa) were established. The width of bed preparations varied: 6 ft for the 1200-1800 tpa treatments, 8 ft for the 600 and 900 tpa plots, and 12 ft for the 300 tpa treatment.

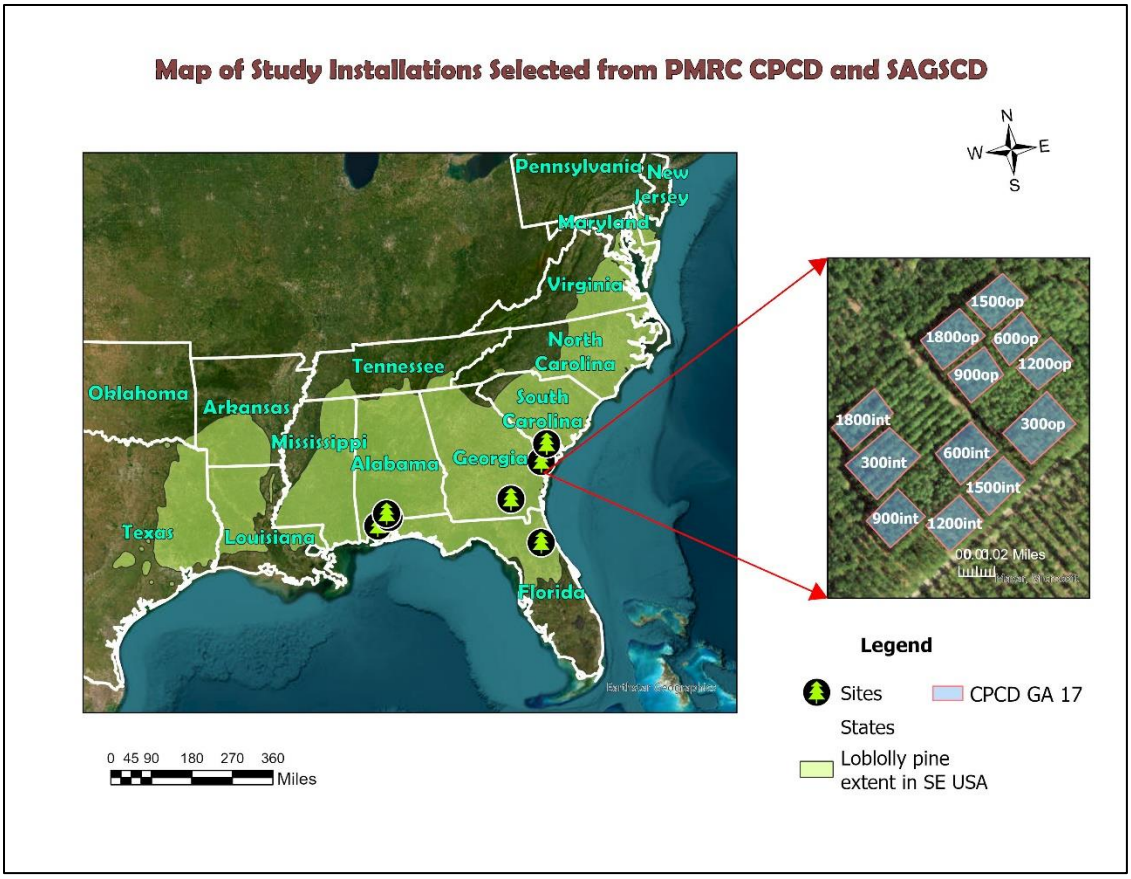

Figure 1. 1 Loblolly pine plantations in SE USA with selected installations from CPCD and SAGSCD studies of PMRC. Each tree icon location corresponds to an installation with 12 plots with different TPA and treatments, either intensive or operations

CHAPTER 1

ASSESSING AN OPTIMAL LIDAR-DERIVED TREE HEIGHTS METHOD

1. BACKGROUND:

The United States is the largest producer of industrial roundwood, contributing to 17% of the global production share. Notably, only 9% of the country's total forested areas are actively managed. Despite the relatively small proportion of managed forests, they play a substantial role, contributing 41% to the nation's industrial roundwood production FAO (2015); (Oswalt et al., 2014). One of the most economically significant tree species for roundwood production is the Loblolly pine (*Pinus taeda L.*), mainly cultivated in the southern United States (Jeffrey P. Prestemon, 2002; Zalesny et al., 2011). This species has a medium lifespan, moderate tolerance for shade, and grows rapidly in its early stages. Notably, this species shows favorable responses to silvicultural treatments and can be managed in even-aged or uneven-aged stands, as well as through artificial regeneration in plantations. Its natural habitat spans 14 states, extending from southern New Jersey down to central Florida and westward to eastern Texas (Little & Viereck, 1971).

Across most of the geographic range of Loblolly pine, the climate ranges from humid, warm-temperate with long, hot summers to mild winters. The primary factor constraining the species expansion to the north is likely the presence of low winter temperatures, leading to damage from ice, snow, sleet, and cold stress during flowering (Fowells, 1965). Compared to many

hardwood competitors, Loblolly pine demonstrates remarkable growth rates, often achieving growth rates that are two to three times higher on numerous sites (Wahlenberg, 1960).

The United States holds a significant position as a major consumer of various wood products, including industrial roundwood (18%), sawnwood (22%), wood-based panels (13%), recovered paper (12%), and paper and paperboard (16%) (Delton Alderman, 2022). Given this significant demand, forest managers must approach forest management decisions with seriousness and precision, recognizing the importance of their roles in sustaining these vital resources. To facilitate these decisions, large-scale forest inventory becomes a critical tool for forest plantation managers, enabling them to gather essential information about forest cover, growth, yield, land attributes, and resource allocation for their plantations (Roise et al., 2016; Silva et al., 2017a; Wulder et al., 2012). As forest inventory attributes are dynamic and keep changing, it is important to predict and project how trees will grow in the future. (Eugene & E., 1983). Using forest's growth and yield models for predicting and projecting forested stands has been in practice for decades (Burkhart & Tomé, 2012). These models are indispensable tools for managers when making decisions regarding intensively managed plantations (Avery & Burkhart, 2015; Weiskittel, 2011). Traditionally, growth and yield models are developed through the utilization of extensive historical data, employing statistical methods (Porte & Bartelink, 2002; Weiskittel, 2011). These models are available for various forest types, including even-aged and uneven-aged stands, as well as single-species and mixed-species forests. They have the capacity to produce results at different levels, ranging from individual tree predictions (Clutter & Allison, 1974) to whole stand projections (Buckman, 1962). Nevertheless, it's important to note that these models are rooted in empirical data and thus are best suited for stand growth conditions similar to those under which they were originally formulated (Miehle et al., 2009; Monserud, 2003). Each model has its own

set of advantages and limitations. While whole-stand models often yield accurate results at the stand level, they may lack information about stand structures. Conversely, detailed data from individual-tree models and size-class models can provide stand-level outputs but may introduce more imprecision (Jianhua & Cao, 2006). There are hundreds of simulation models which can provide forest managers the predictions of forest growth and yield (Ashton & Liu, 1995). Nevertheless, among the numerous available models, it is challenging to validate or determine the best representation of reality (Robinson & Monserud, 2003). Therefore, selecting the appropriate model hinges on the specific needs and objectives of the forest manager (Buchman & Shifley, 1983).

Diameter at Breast Height (DBH) and tree height are two primary predictors for calculating and explaining tree variability in growth and yield models (Domke et al., 2012; Schumacher & Hall, 1933; Van Deusen, Sullivan, & Matvey, 1981). However, the measurement of tree height in the field presents more significant challenges, primarily due to its susceptibility to various factors. These factors include the observer's position, viewing angle, level of experience, and the presence of obstructing trees that can hinder precise measurements. This inherent complexity introduces a higher level of potential bias when compared to the relatively more straightforward process of measuring diameters. For instance, Rennie (1979) documented errors in the range of 0.67 to 1.10 meters when using conventional hypsometers for tree height measurements in loblolly plantations. Numerous researchers have reported instances where foresters frequently resort to imprecise, unreliable, and biased estimates, resulting in elevated measurement errors within growth and yield models that incorporate tree height as a predictive factor in their equations (Avery & Burkhart, 2015; Yang & Burkhart, 2020).

To address this challenge, a commonly used approach is mapping the spatial growth of stands by integrating forest inventory data with remotely sensed data. Light Detection and Ranging (LiDAR) is an active remote sensing system that generates an accurate 3-D point cloud that defines vertical and horizontal forest structures that can be used in forest inventories (Hyyppa et al., 2001; Marczak et al., 2020; Mohan et al., 2019; Zimble et al., 2003). Moreover, it provides the possibility of decreasing the number of required sampling (Montaghi et al., 2013), and the forest attributes estimates with LiDAR are efficient and accurate compared to traditional inventory techniques (Matti Maltamo, 2014; Miehle et al., 2009; Woods et al., 2011). Leveraging LiDAR data provides an opportunity to enhance forest attributes information, thereby improving growth and yield models for sustainable forest planning and management (Tompalski et al., 2018).

There are two types of aerial LiDAR systems: a) Airborne LiDAR Scanner (ALS) and b) Unmanned Aerial Vehicle (UAV) based LiDAR. ALS technology has found extensive application in a wide array of research endeavors. Studies utilizing ALS have spanned various domains, including but not limited to estimating biomass, predicting volume, conducting comprehensive mapping of ecosystem-wide vegetation parameters, and quantifying undergrowth vegetation (Bortolot & Wynne, 2005; Edson & Wing, 2011; Green et al., 2020a; Green et al., 2022; Silva et al., 2017a). The robustness and versatility of ALS have enabled researchers to explore multifaceted dimensions of forest ecosystems. However, the use of ALS data has been associated with certain challenges, such as high data acquisition costs, limitations imposed by flight duration, and low point density of returns, which have constrained the scope of ALS-based studies. The emergence of UAV as an alternative aerial platform presents a notable shift in forest data analysis. UAV offers the distinct advantage of operating without human pilots on board, thereby enhancing safety and expanding data collection opportunities. A key distinguishing feature of UAV-based LiDAR

systems, when compared to ALS, is their cost-effectiveness and the ability to produce high-resolution outputs (Dalla Corte et al., 2020). This unique combination addresses the challenges associated with data acquisition expenses while simultaneously improving the quality of collected data. The UAV stands out as an ideal platform for LiDAR data collection due to its cost-effectiveness, user-friendly interface, and automated workflow, offering high resolution at reasonable expense. However, various factors can impact data quality and the most effective practices (Watts, Ambrosia, & Hinkley, 2012). Researchers across disciplines have delved into conditions affecting data capture and processing, potentially compromising positional certainty or reliability (Colomina & Molina, 2014). Issues like DEM accuracy and the impact of strong winds during flights, leading to data point gaps as drones deviate from the flight line, are challenges that need attention when utilizing (Scicluna, Sant, & Farrugia, 2023) UAVs for studies. It is crucial to thoroughly assess and address these issues to ensure the quality of the data collected. In addition to aerial LiDAR, various Terrestrial LiDAR Scanner (TLS) also offer an enhanced solution for obtaining comprehensive under the canopy data for assessing different tree attributes (Merlijn Simonse; Simonse et al., 2003) and attributes related to the forest environment and inventory (Bauwens et al., 2016). These attributes commonly derived from each geolocated laser pulse within a laser point cloud encompass a wide range of characteristics. They include attributes such as intensity, return number, count of returns, point classification values, points located at the edge of the flight line, RGB (red, green, and blue) values, GPS time, scan angle, and scan direction.

Recently, the application of LiDAR for forest measurements has experienced rapid growth. Studies focused on estimating and predicting various forest biophysical variables at the plot level, including maximum canopy height, mean canopy height, Lorey's height, basal area, crown closure, diameter at breast height (DBH), biomass, leaf area index (LAI), and volume, have predominantly

relied on establishing empirical relationships between various LiDAR canopy height and density metrics and the biophysical variables of interest (Dean et al., 2009; Hilker, Wulder, & Coops, 2008; Lim et al., 2003b; Lim & Treitz, 2004; Næsset, 2002; Nelson, 1997; Nelson, Oderwald, & Gregoire, 1997; Peduzzi et al., 2012; Popescu, 2007; Ruiz et al., 2014). Furthermore, the quality of LiDAR elevation data is contingent on several factors, including instrumental, methodological, and site-specific considerations. Developing effective methods to mitigate bias in LiDAR data has always been a challenge due to the numerous factors contributing to underestimation or overestimation (Hodgson et al., 2003; Hyyppae et al., 2000; Sithole & Vosselman, 2004).

Numerous studies have explored various methodologies for extracting canopy heights from LiDAR data. Generally, two approaches can be used to extract metrics from LiDAR data for volume prediction models: (a) echo-based metrics and (b) canopy height model (CHM)-based metrics. The first one characterizes forest structure by means of a 3D point cloud, whereas a CHM is a raster surface model, is a type of raster surface model, similar in nature to a digital elevation model (DEM). It is created by interpolating data points collected from the upper surface of the canopy. CHM metrics provide only a limited number of metrics, such as minimum, maximum, average, and standard deviation values of height (Barbati et al., 2009).

On the other hand, echo-based metrics offer a wider range of metrics, including minimum, mean, maximum, standard deviation, skewness, kurtosis, coefficient of variation, and various distribution percentiles (Gobakken & Næsset, 2008; Lim et al., 2003a; Lim et al., 2003b; Næsset, 2002). Additionally, metrics like canopy relief ratio have been derived from echo-based data (Alistair et al., 2009). Studies have highlighted the significance of these metrics. For example, Yu et al. (2004) it was observed that differences in mean CHM height estimates from field data collected 21 months apart ranged from 10 to 15 cm. Similarly, Hopkinson, Chasmer and Hall

(2008) found that the 100th height percentile offered the most accurate direct estimation of forest growth when compared to field measurements. Another method for extracting height information from LiDAR data involves utilizing LiDAR pixel_metrics in R (R Core Team, 2022). In this approach, statistical calculations are performed on the point cloud data within each pixel. These statistics can include metrics like the mean height of returns, standard deviation of return heights, return height percentiles, and more. The plots of interest are then subdivided into multiple pixels according to the desired resolution, which is determined based on the point density of the available LiDAR data. (Lamb et al., 2018). Despite significant advancements in these methods, a comprehensive comparative analysis aimed at identifying the most accurate method for loblolly plantation has not been conducted yet.

Furthermore, the point densities and spatial distribution of 3D points within LiDAR data significantly impact the accuracy of derived Digital Elevation Models (DEMs) and subsequently affect canopy height estimations. Research has demonstrated that very low point densities during LiDAR data acquisition can compromise DEM quality as only a few pulses reach the ground and are available for DEM construction (Hansen, Gobakken, & Næsset, 2015). Conversely, high-density LiDAR data ensures good point density and elevational accuracy (Liu et al., 2007; Silva et al., 2017b). There are studies comparing the effect of point densities in plot-level and individual tree detection inventories in loblolly pine plantations. For instance, Green et al. (2020b) found that lower LiDAR point-cloud densities and DEM spatial resolutions had minimal effects on the precision of total volume estimates for small area estimation. However, Sumnall et al. (2022) summarized the impact of UAV pulse density (.25, .5, 1, 5, 10, 50, 100, and 300 pulses/m^2) on the ability to delineate individual tree crowns (ITCs) and plot-level leaf area estimates. They concluded that low point density LiDAR could estimate plot-level metrics, but accuracy decreased

for individual tree-level crown detection in loblolly pine plantations. Given the expanding adoption of LiDAR technology in forest plantations for tree height estimation, there is a growing need to evaluate and identify the optimal method for estimating tree heights with an appropriate point density that is insignificantly different from field measurements.

2. GOALS, OBJECTIVES, AND HYPOTHESIS

The primary goal of this study is to evaluate the potential of employing LiDAR-derived tree heights from two distinct years, along with field inventories and advanced statistical models, to improve the accuracy and effectiveness of growth and yield models for loblolly pine plantations. The specific objectives of the study are:

- To evaluate differences in field measurement heights and LiDAR extracted heights and identify the optimal method to generate dominant height from LiDAR.
- To evaluate if tree heights extracted from low point density and high point density LiDAR show differences with respect to heights measured from the ground.

3. MATERIALS AND METHODOLOGY

Field Measurements:

Diameter at Breast Height (DBH) was measured for each tree using diameter tape within the measurement plot, with precision to the nearest 1/10th of an inch. Additionally, total tree height in ft, along with the height to the live crown, was recorded for every alternate tree in the plot. For trees that were not directly measured for total height, precise estimates were calculated using the following height-diameter regression equation by Schumacher and Hall (1933):

$$HT = 4.5 + a * e^{-b/}_{DBH} \quad (1)$$

where HT = total tree height, DBH is tree diameter at breast height, and a and b are parameters to be estimated from each plot at each measurement. After estimating the total height for all the trees within the study area, the next step involved calculating the dominant height. This was achieved by determining the average height of the dominant and codominant trees within each plot. Specifically, these were the trees with a Diameter at Breast Height (DBH) greater than the quadratic mean diameter.

Individual tree, outside bark cubic foot volumes and green weights with bark were calculated using the following equations from Pienaar, Burgan and Rheney (1987):

$$VOB = 0.00145519 DBH^{1.086054} HT^{1.221965} \quad (2)$$

$$GWOB = 0.0740959 DBH^{1.0829983} HT^{1.247669} \quad (3)$$

Table 1: Study installation and plot details. SAGSCD has three sites, having 2010 data for Site 2 and 2013 for year 1 data for three and four installations. Year 2 data for Site 2 is from 2017 whereas for Site 3 and 4 have data from 2021. Similarly, for year 3, all three installations have data from the year 2023. For Year 1, the total plots were 84, for year 2, 75, and for year 3, 68 plots.

Study AREA	INST	n (P/A) Year1	n (P/A) Year 2	n (P/U) Year 3	Year1	Year2	Year3	AGE 1	AGE 2	AGE 3
SAGS Est. 1996/97	2	12	10	9	2010	2017	2023	12	21	24
	3	12	12	12	2013	2021	2023	15	25	24
	4	12	12	12	2013	2021	2023	15	25	24
CPCD Est. 1998/9	6	12	11	10	2010	2019	2023	15	23	27
	12	12	12	12	2010	2018	2023	15	24	27
	13	12	8	4	2012	2019	2023	17	24	27
	17	12	10	9	2010	2018	2023	15	24	27
Total Plots		84	75	68	P/A= plot and ALS					
					P/U= plot and UAV					

LiDAR data:

LiDAR data were collected from two types of aerial platforms: a) ALS and b) UAV.

Airborne Laser Scanner (ALS):

We obtained two distinct sets of ALS data from the same year as the field inventory data using the USGS LidarExplorer . It's important to note that each data set corresponds to different projects conducted in various states. In year 1, the point density of the data varied between 1.58 and 7.20 points per square meter. However, in year 2, the ALS data exhibited higher point densities, ranging from 3.83 to 44.95 points per square meter, depending on the specific study sites.

Table 1.1 Details of ALS LiDAR data projects for years 1 and 2, downloaded from USGS LiDAR Explorer

Study	Site	Y1	LiDAR Project	Y2	LiDAR Project
SAGSCG	2	2010	AL Mobile Bay 2010	2017	AL_25_County_Lidar_2017
	3	2013	AL_EscambiaCo_2013	2022	AL_CoffeeDaleGenevaEscambia_2021
	4	2013	AL_EscambiaCo_2013	2022	AL_CoffeeDaleGenevaEscambia_2021
CPCD	6	2010	HamptonCo_2010	2020	SC_SavannahPeeDee_2019
	12	2010	GA_Okefenokee_2010	2019	GA_Statewide_2018
	13	2012	FL_StJohnsRiver_WMD_2012	2019	FL_Peninsular_2018
	17	2010	GA_Effingham_Screven_Bulloch2010	2019	GA_Statewide_2018

Processing:

We obtained the data by using a boundary shapefile to identify and download matching tiles containing LiDAR datasets in the LAS file format. These tiles originally had differing projection systems. To ensure consistency, we utilized LASTOOLS, specifically the 'las2las' tool in the command prompt, to reproject them into the NAD83 (National Spatial Reference System 2011) EPSG:6350 coordinate system. This choice of projection system was made to ensure compatibility with all the states involved in the study.

The preprocessing of the LiDAR data consisted of several steps and lidR package (Roussel et al., 2020) was used for processing. Initially, we removed extreme observations, which were significantly higher than the median elevation of neighboring points or isolated points resulting from the backscatter of flying objects. Subsequently, we generated a digital elevation model (DEM) with a resolution of five meters by classifying ground points using the universal Kriging algorithm. We opted for Kriging interpolation because it is better suited for LiDAR data with reduced point densities compared to other techniques (Chu et al., 2014). After the DEM, normalization was done using "normalize_height" function, it is a process of subtracting the DEM derived from the LiDAR data to the point cloud data. This brings consistency and uniformity to the data by removing or mitigating variations caused by factors such as terrain, sensor characteristics, and data acquisition conditions. After normalization, a normalized LAS file was clipped to each plot level using shapefiles (vector file defining boundary of the plot perimeter in field).

Afterwards, we created a Canopy Height Model (CHM) with a resolution of 5 meters using the dsmtin algorithm within the 'rasterize_canopy' function of the lidR package in R. This algorithm employs Delaunay triangulation of first returns with linear interpolation within each triangle. After the CHM raster was generated, we used its mean height as the height measurement for the entire plot.

LiDAR forest metrics were computed in two ways: directly from the point cloud and by using pixels to calculate LiDAR height and density metrics. Traditional LiDAR metrics were computed for the field plots in R These metrics included percentiles of height from the 1st percentile to the 99th percentile, median height, maximum and minimum heights, as well as the count of returns above the mean, mode, and various other thresholds. Similar metrics were derived

using the 'pixel_metrics' function from the lidR library (Roussel et al., 2020), with an ALS pixel resolution of 5 meters.

In our data height extraction process, aimed at comparing the dominant height of trees in the field with the height measurements obtained through LiDAR technology, we undertook a series of precise steps. To tailor our LiDAR data analysis to the unique requirements of our research, we made custom adjustments to the pixel_metrics. These modifications were vital to ensure that we extracted the height information most pertinent to our study. Subsequently, we implemented a filtering procedure on the normalized LAS files. This filtering process was instrumental in selecting the heights of the dominant trees, effectively capturing the tallest trees in the dataset. We employed the 95th percentile as the threshold to achieve this. Following this filtering process, we calculated several key height percentiles, specifically the 95th, 99th, and the HMAX values. These calculations were carried out using the customized pixel_metrics, enabling us to gain detailed insights into the distribution of tree heights within each plot. By repeating these meticulous steps for each individual plot in our study, we derived plot-level LiDAR pixel heights. This resulted in a dataset that provided precise height information for each plot, with a particular emphasis on the tallest trees within each plot.

Unmanned Air Vehicle (UAV):

The UAV-LiDAR data was obtained in 2022 dormant season, with the Headwall UAV system. The Headwall unit comprises a DJI M600 Pro UAV, a Velodyne VLP-16 Puck (Velodyne LiDAR Inc., Morgan Hill, CA, USA) LiDAR sensor, and an Inertial Measurement Unit (IMU). The VLP-16 Puke LITE, weighing 590 g, is a Light Detection and Ranging (LiDAR) featuring 16 channels. The unit can measure up to 300,000 points per second in dual return mode within a maximum range of 100 m. The device uses a continuous wavelength of 903 nm (near infrared) to

measure distances with a range accuracy of ±3 cm. The VLP-16 has a field of view of 360° × 30° with a vertical angular resolution of 2° and a horizontal angular resolution of 0.1°–0.4°. The VLP-16 analyzes multiple returns and reports either the strongest, last, or both returns. In this study, we used both return modes, where the sensor records two returns (first and last) when the distance between two objects situated within the same laser beam is greater than 1m. The flying height was 80 m above the ground at a speed of 5/m^2 and an approximate horizontal distance between the adjacent flight lines of 20 m, producing a high-density LiDAR point cloud The UAV flight lines provide redundant coverage in the area (overlap of 40%). The point density of LiDAR point cloud was in range of 359.40 to 551.13 points/m^2, depending on specific study sites.

Processing:

The initial processing of UAV-lidar data commenced with the classification of returns into ground and non-ground categories, achieved through the application of a cloth simulation filter (CSF) following the approach proposed by Zhang et al. (2016). While collecting data, the drone roll, pitch, and yaw may have influenced the alignment and stability of the LiDAR sensor. These rotational movements could have introduced inaccuracies in our acquired LiDAR data, leading to variations in the recorded elevation values. To ensure accuracy, we implemented several measures. Firstly, data collection occurred in favorable weather conditions, avoiding windy weather. Secondly, our calibration process involved meticulous parameter selection. Additionally, after data collection, the point cloud underwent comprehensive scrutiny using both CloudCompare software and ArcPro GIS. Once we confirmed the absence of height differences in our data then we executed a sequence of processing steps analogous to those employed for ALS data, starting with the generation of a Digital Elevation Model (DEM), data normalization, and then clipping of LAS

files to the plot dimensions. Notably, the UAV-lidar data has a higher point cloud resolution in comparison to ALS, enabling us to create DEMs, Canopy Height Models (CHMs), and pixel-level metrics at a higher level of detail. The DEM and CHM were generated at a resolution of 0.5 meters, while pixel-level metrics were computed at a 1-meter. We conducted a thorough examination for potential errors that might arise from UAV factors. First, including the possibility of gaps in DEM due to the wind effect on our lightweight UAV-lidar system. Fortunately, the DEM did not show any significant issues. The remaining processing steps and resulting products were consistent with those employed for ALS data processing.

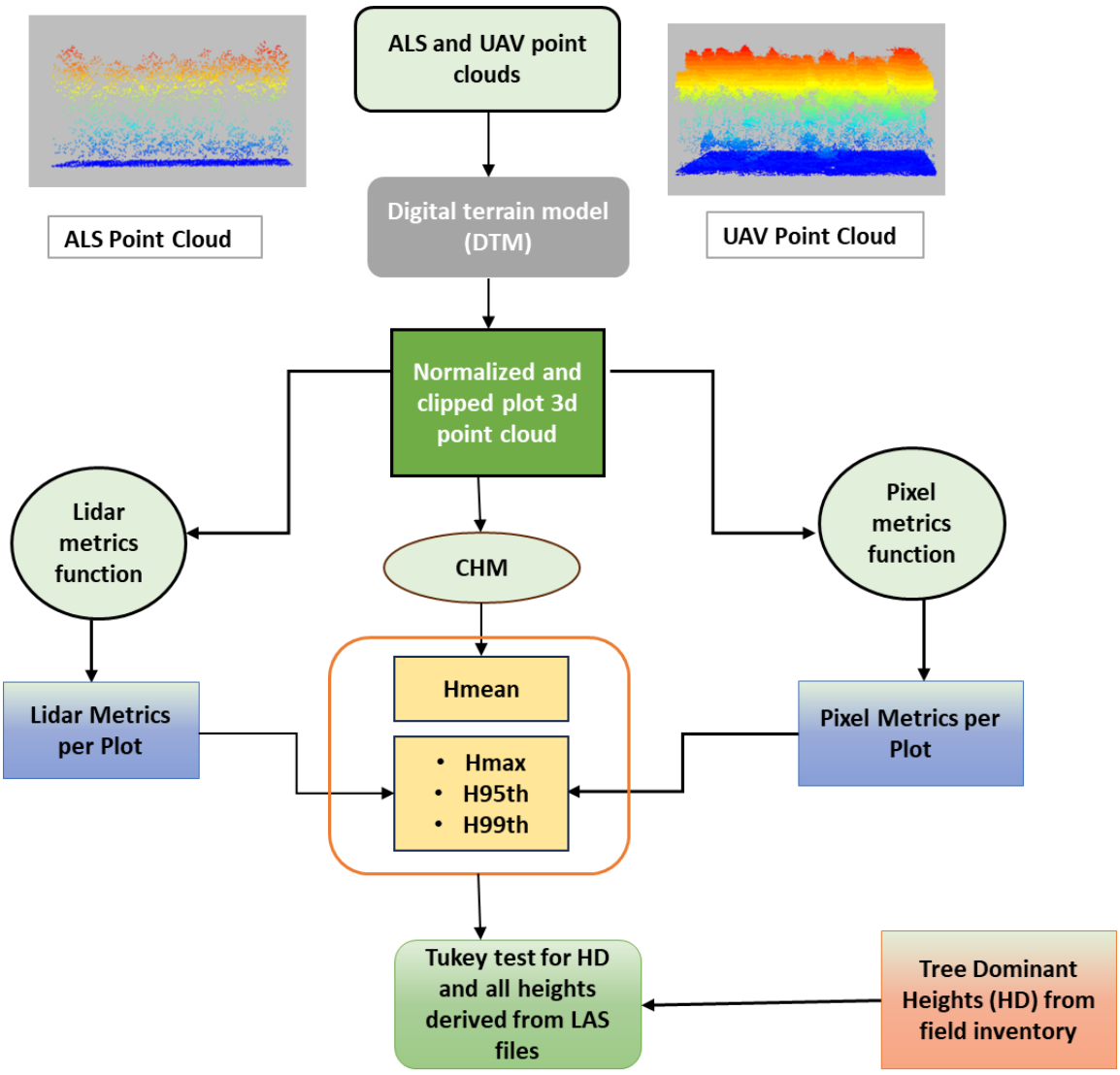

Figure 1. 2 Flowchart of LiDAR data extraction with different methods

Statistical Analysis:

All analysis conducted for this study were performed using R Programming (R Core Team, 2022) and JMP (JMP®17, 2022). Most of the graphics were developed using the packages ggplot2 (Wickham, 2011), lattice (Sarkar, 2008), and other.

Analysis of heights comparison:

Tukey's HSD test was selected as the preferred method for comparing tree heights across different plot categories defined by Trees Per Acre (TPA) and various LiDAR heights extraction techniques. This choice was driven by its unique advantages, including the ability to conduct specific pair-wise comparisons among groups, effective control over the family-wise error rate, accommodation of multiple comparisons, enhancement of statistical power, straightforward interpretability, and robustness even in scenarios involving unequal variances or unbalanced sample sizes. These qualities made it the most appropriate choice for our comprehensive comparison. Consequently, we employed the Tukey HSD test for the mean comparison of tree heights within the JMP software. JMP utilized graphical representations for ease of understanding and visual clarity. In the generated graph, there are vertically arranged circles on the right side, with each circle corresponding to the group mean or average for a specific category. Higher circles indicate higher means, while lower ones represent lower means. The horizontal spacing between these circles plays a vital role in the interpretation. Non-overlapping circles indicate statistically significant differences between group means, while overlapping circles suggest no significant difference. Additionally, above these circles, there are letters that denote which groups share means that are not significantly different (groups with the same letter) or significantly different (groups with different letters) from each other.

Bootstrapping Tukey HSD Height:

Bootstrapping is a computational resampling technique that utilizes numerous iterations to approximate the distribution of a statistical measure. This method involves repeatedly drawing samples from the data with replacements to generate empirical estimates of the entire sampling distribution of the statistic. The Tukey test assumes homogeneity of variances (equal population variances) and a normal distribution of data. If these assumptions are violated for some pairwise comparison in our analysis, Tukey's test results may lack reliability. For this, we will use bootstrapping. The strength of bootstrapping lies in its non-parametric nature, circumventing the need for these assumptions and enhancing robustness when working with not normally distributed data. Furthermore, bootstrapping exhibits reduced sensitivity to outliers compared to traditional parametric methods (Mooney, Duval, & Duvall, 1993). By resampling with replacement, extreme values would have less influence on the result which will lead to more robust statistical inferences for our analysis.

In our analysis using R, we utilized the "boot" library to perform bootstrap resampling for the Tukey HSD test. We performed 1000 iterations, comparing mean differences among different trees per acre treatments (TPA). This involved repeatedly sampling from our dataset with replacement and applying Tukey's HSD test to estimate mean differences. After 1000 iterations, we extracted the p-values associated with the mean comparisons. Then, we calculated the percentage of times when pairs of fields and LiDAR mean values for each TPA were not significantly different and the percentage when they were significantly different. This approach allowed us to understand the variability in mean differences and provided insights into the significance of these differences across multiple iterations.

4. RESULTS:

Plots were categorized based on varying Plot Level Trees Per Acre (PLTPA) levels, allowing for a height comparison. Dominant heights for each plot were determined using data from CPCD and SAGSCD measurements, representing the average height of trees with diameters exceeding the arithmetic mean DBH. The findings are categorized by the distinct LiDAR types employed, which include ALS and UAV-LiDAR.

Table 1.2 Descriptive statistics from field measurements height in ft showing Mean, Standard Deviation (SD), Minimum (Min) and Maximum (Max) for respective years 1, 2 and 3 with different PLTPA.

	Year 1 (ft)				**Year 2 (ft)**				**Year 3 (ft)**			
PLTPA	Mean	SD	Min	Max	Mean	SD	Min	Max	Mean	SD	Min	Max
300	64.48	9.01	48.10	77.80	90.45	5.64	79.00	97.20	94.41	4.75	86.80	103.30
600	62.79	9.66	42.89	75.78	87.51	8.38	66.26	96.67	90.56	7.87	71.37	98.82
900	60.31	9.74	39.77	74.03	84.07	9.08	61.50	93.75	88.64	9.33	64.89	103.00
1200	59.76	10.05	38.03	72.54	84.02	9.78	59.77	95.50	86.76	9.36	64.58	97.69
1500	58.43	9.90	36.95	72.45	82.09	9.85	60.55	94.71	86.45	10.23	64.58	98.80
1800	58.99	10.43	37.35	73.71	80.90	10.58	56.88	94.54	84.16	9.65	61.29	93.58

Table 1.3 shows the field dominant heights in the context of PLTPA at different levels over the course of three years. The data reveals significant changes over these three years. In the first year, for PLTPA 300, the average field height was 64.48 ft, with some variability (Standard Deviation, SD, of 9.01, and a range from 48.1 to 77.8). But in the second year, this average increased to 90.45 ft (SD 5.64, Min 79, Max 97.2), and it continued to rise in the third year, reaching 94.41 ft (SD 4.75, Min 86.8, Max 103.3). Likewise, considering PLTPA 600, Year 1 showed a mean field height of 62.79 ft (SD 9.66, Min 42.89, Max 75.78). In Year 2, there was a

substantial increase to 87.51ft (SD 8.38, Min 66.26, Max 96.67), and Year 3 witnessed a further rise to 90.56 ft (SD 7.87, Min 71.37, Max 98.82). For PLTPA 900, the initial year recorded an average field height of 60.31 (SD 9.74, Min 39.77, Max 74.03), which rose to 84.07 ft (SD 9.08, Min 61.5, Max 93.75) in Year 2, and eventually increased to 88.64 (SD 9.33, Min 64.89, Max 103) in Year 3. Year 1 showed a mean field height of 59.76 ft (SD 10.05, Min 38.03, Max 72.54) for PLTPA 1200, which escalated to 84.02 ft (SD 9.78, Min 59.77, Max 95.5) in Year 2, and further increased to 86.76 ft (SD 9.36, Min 64.58, Max 97.69) in Year 3. In Year 1, the field height for PLTPA 1500 had an average of 58.43 ft (SD 9.9, Min 36.95, Max 72.45). Subsequently, in Year 2, the mean reached 82.09 (SD 9.85, Min 60.55, Max 94.71), and increased to 86.45 ft (SD 10.23, Min 64.58, Max 98.8) in Year 3. As for PLTPA 1800, Year 1 reported a mean field height of 58.99 ft (SD 10.43, Min 37.35, Max 73.71). This mean rose to 80.9 ft (SD 10.58, Min 56.88, Max 94.54) in Year 2, and further increased to 84.16 ft (SD 9.65, Min 61.29, Max 93.58) in Year 3.

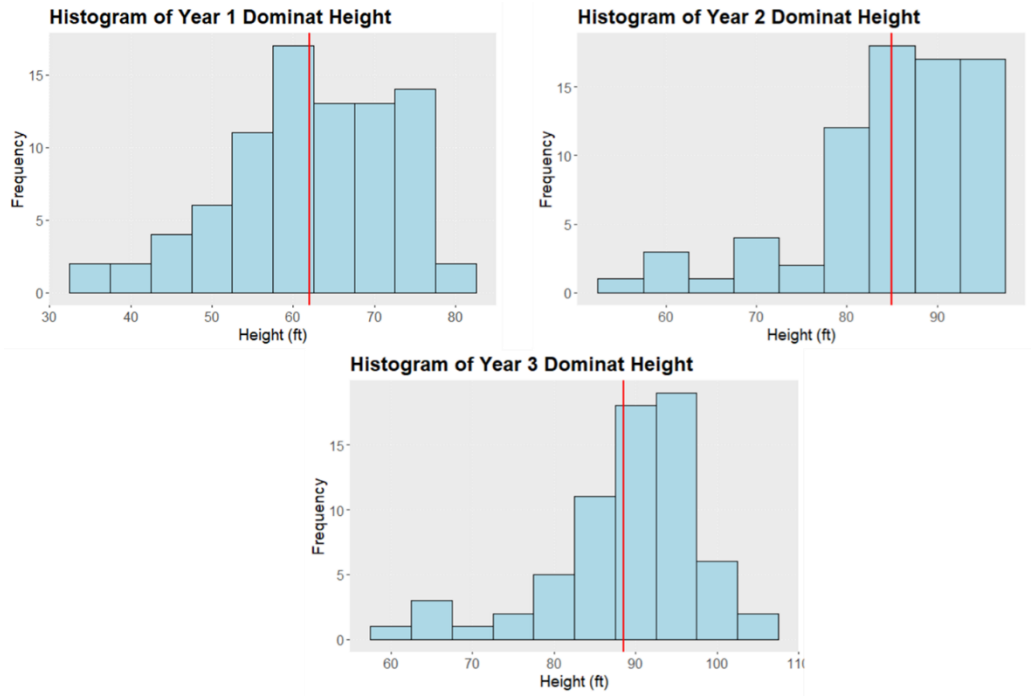

Figure 1. 3 Histogram depicting field dominant heights for all three years, with the red line representing the average height value for that specific year across all plots

Airborne Laser Scanner (ALS)

Mean comparison using Field Dominant Height and Canopy Height Model

Table 1. 3 Tukey means comparison of field dominant height with heights derived from Canopy Height Model for both year 1 and year 2.

Year 1							**Year 2**					
		HD (ft)		**CHM (ft)**				**HD (ft)**		**CHM (ft)**		
PLTPA	**N (plots)**	**Mean**	**Std Dev**	**Mean**	**Std Dev**	**P-Value**	**N (plots)**	**Mean**	**Std Dev**	**Mean**	**Std Dev**	**P-Value**
300	14	65.40	8.73	57.45	8.45		12	89.92	6.98	79.68	15.45	
600	14	64.01	10.21	57.00	9.44		14	86.63	10.00	80.34	8.17	
900	14	61.49	10.44	55.17	8.96		14	83.26	10.90	77.53	8.97	
1200	14	61.22	10.65	54.89	8.76	0.03*	13	81.98	12.10	76.79	9.08	0.05
1500	14	59.75	10.48	55.49	8.97		12	80.94	12.10	77.49	9.71	
1800	14	60.23	10.31	55.36	9.55		11	80.07	12.10	76.57	9.85	

Means comparison using Field Dominant Height and lidar_metrics:

Table 1.4 Tukey means comparison of field dominant height with heights derived from lidar_metrics for year 1 for all treatments or PLTPA.

Year 1									
		HD (ft)		Metrics H95TH (ft)			Metrics H99TH (ft)		
PLTPA	N (plots)	Mean	Std Dev	Mean	Std Dev	P-Value	Mean	Std Dev	P-Value
300	14	65.4	8.73	57.48	7.6		60.61	7.54	
600	14	64.01	10.21	57.41	8.66		60.22	8.77	
900	14	61.49	10.44	55.72	8.54		58.31	8.73	
1200	14	61.22	10.65	55	8.42		57.69	8.48	
1500	14	59.75	10.48	55.22	8.73	0.03*	58.05	8.89	0.54
1800	14	60.23	10.31	55.58	8.91		58.26	8.93	

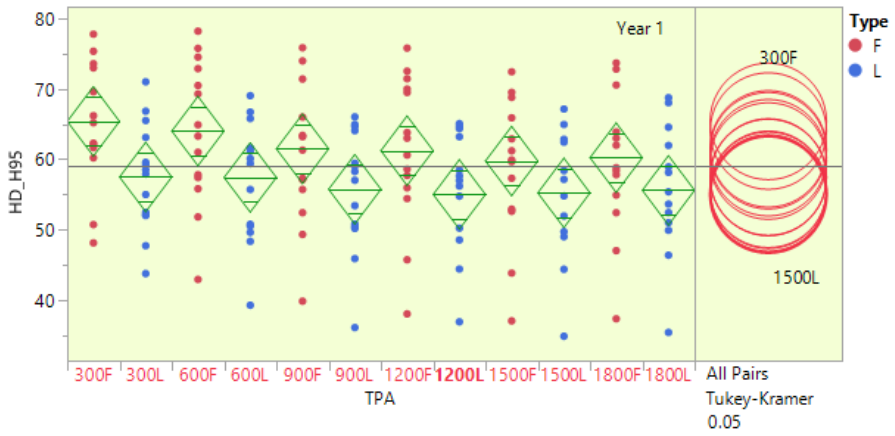

Figure 1. 4 Tukey test plot of field HD and lidar_metrics H95th percentile in ft for Year 1 by planting density. The circles in the right side denote the range of heights. The circle on the right side denotes the range of height in each plot.

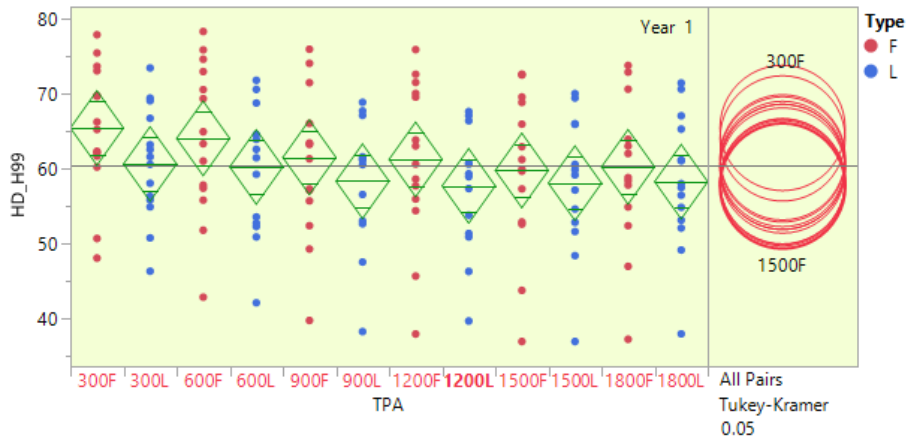

Figure 1. 5 Tukey test plot of field HD and lidar_metrics H99th percentile in ft for Year 1 by planting density. The circles in the right side denote the range of heights.

Table 1. 5 Tukey means comparison of field dominant height with heights derived from lidar_metrics for year 2 for all treatments or PLTPA

Year 2									
		HD (ft)		Metrics H95TH (ft)			Metrics H99TH (ft)		
PLTPA	N (plots)	Mean	Std Dev	Mean	Std Dev	P-Value	Mean	Std Dev	P-Value
300	12	89.92	6.98	86.36	6.85		86.36	6.85	
600	14	86.63	10.03	83.97	7.61		83.97	7.61	
900	14	83.26	10.88	81.09	8.88		81.09	8.88	
1200	13	81.98	12.07	80.02	8.82	0.02*	80.02	8.82	0.21
1500	12	80.94	12.1	80.76	9.38		80.76	9.38	
1800	11	80.07	12.11	79.98	9.94		79.98	9.94	

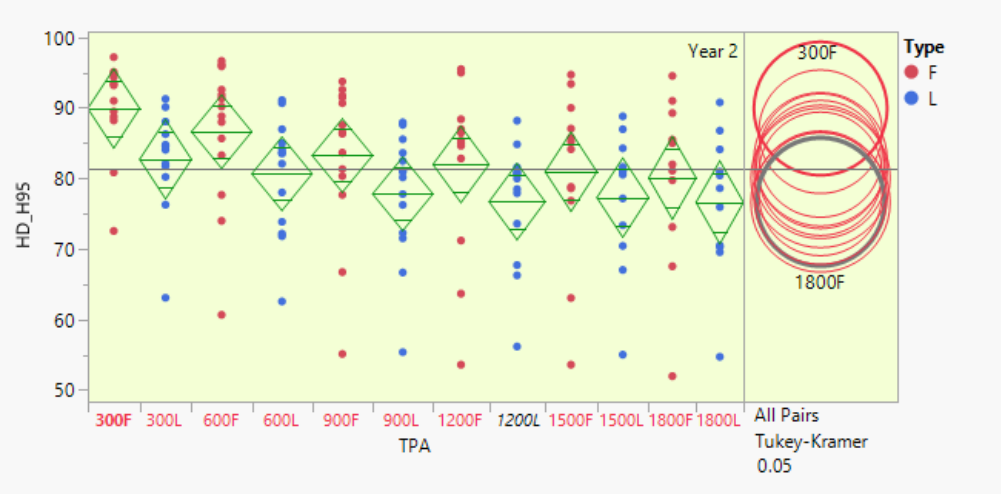

Figure 1. 6 Tukey test plot of field HD and LiDAR_metrics H95th percentile in ft for Year 2 by planting density. The circles in the right side denote the range of heights

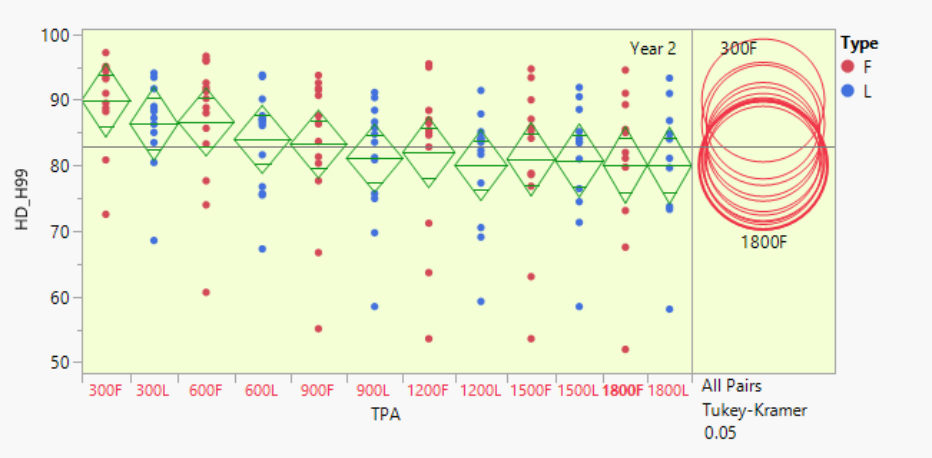

Figure 1. 7 Tukey test plot of field HD and lidar_metrics H99th percentile in ft for Year 2 by planting density. The circles in the right side denote the range of heights

Tables 1.5 and 1.6 provide a comprehensive overview of the Tukey-HSD means comparison results for different PLTPA levels, focusing on the mean heights along with two specific metrics from the lidar_metrics function per plot: H95TH and H99TH. This analysis is conducted over two separate years, Year 1, and Year 2.

Similar to table 1.4, a consistent pattern is observed: lower PLTPA levels are associated with higher average tree heights, while higher PLTPA levels exhibit lower mean tree heights, regardless of whether you're looking at H95TH or H99TH. However, it's important to note that the mean height values derived from the lidar_metrics function are higher than those obtained from CHM. For example, in Year 1, for a PLTPA level of 300, the mean height was 57.48 ft for H95TH and 60.61 ft for H99TH, both of which are higher than the values from CHM.

In Year 1 (Table 5), the P-values indicate that the mean height between HD and H95TH was significantly different (P-Value 0.03*), while H99TH did not show a significant difference (P-Value 0.54). In Year 2 (Table 6), a similar pattern is observed. The P-values suggest that the mean height between HD and H95TH was significantly different (P-Value 0.02*), while there was no significant difference between HD and H99TH (P-Value 0.21). These findings suggest that, in both years, H95TH exhibited significant differences between HD and lidar_metrics data, while H99TH did not. Furthermore, the lidar_metrics data consistently showed higher mean heights compared to CHM.

Mean comparison using Field Dominant Height and pixel_metrics:

Table 1.6 Tukey mean comparison of field dominant height with heights derived from pixel_metrics year 1 for all treatments or PLTPA .

Year 1												
		HD (ft)		Pixel H95TH (ft)			Pixel H99TH (ft)			Pixel Hmax (ft)		
PLTPA	N (plots)	Mean	Std Dev	Mean	Std Dev	P-Value	Mean	Std Dev	P-Value	Mean	Std Dev	P-Value
300	14	65.40	8.73	59.03	7.55		59.39	7.70		59.50	7.77	
600	14	64.01	10.21	58.89	7.73		59.28	7.94		59.39	8.01	
900	14	61.49	10.44	57.88	7.63		58.16	7.76		58.24	7.81	
1200	14	61.22	10.65	57.51	7.59	0.31	57.76	7.73	0.4	57.83	7.76	0.43
1500	14	59.75	10.48	57.05	9.24		57.46	9.04		57.58	8.96	
1800	14	60.23	10.31	57.19	9.35		57.58	9.17		57.70	9.08	

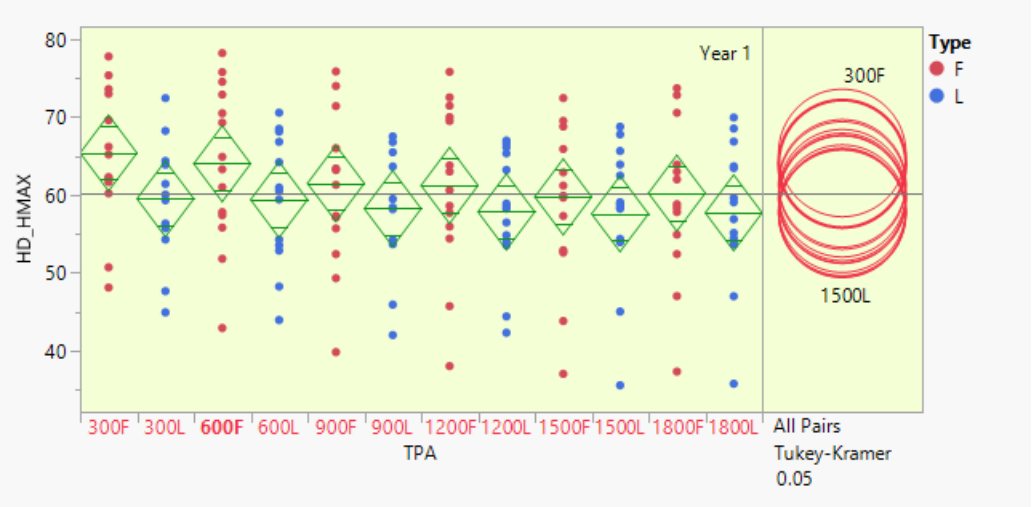

Figure 1. 8 Tukey test plot of field HD and pixel_metrics Hmax percentile in ft for Year 1 by planting density. The circles in the right side denote the range of heights

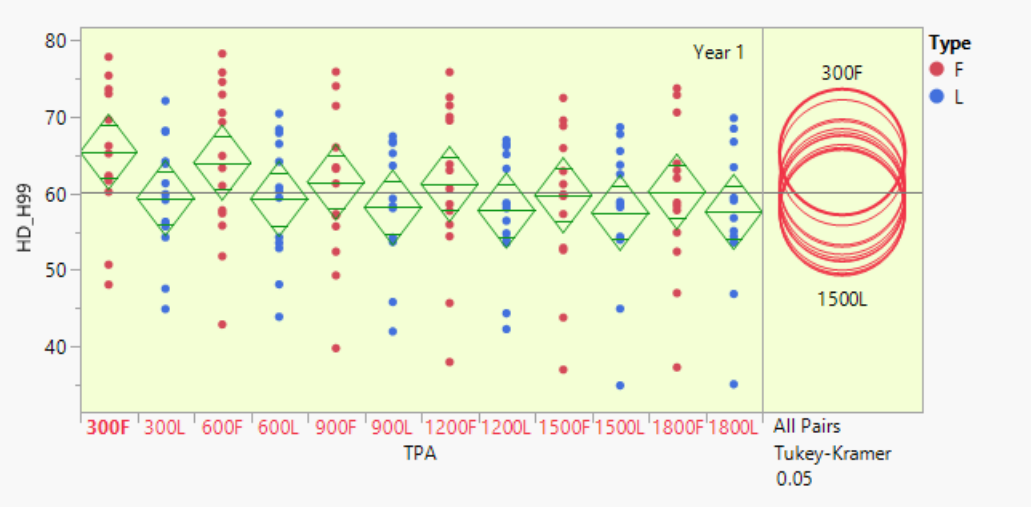

Figure 1. 9 Tukey test plot of field HD and pixel_metrics H99th percentile in ft for Year 1 by planting density. The circles in the right side denote the range of heights

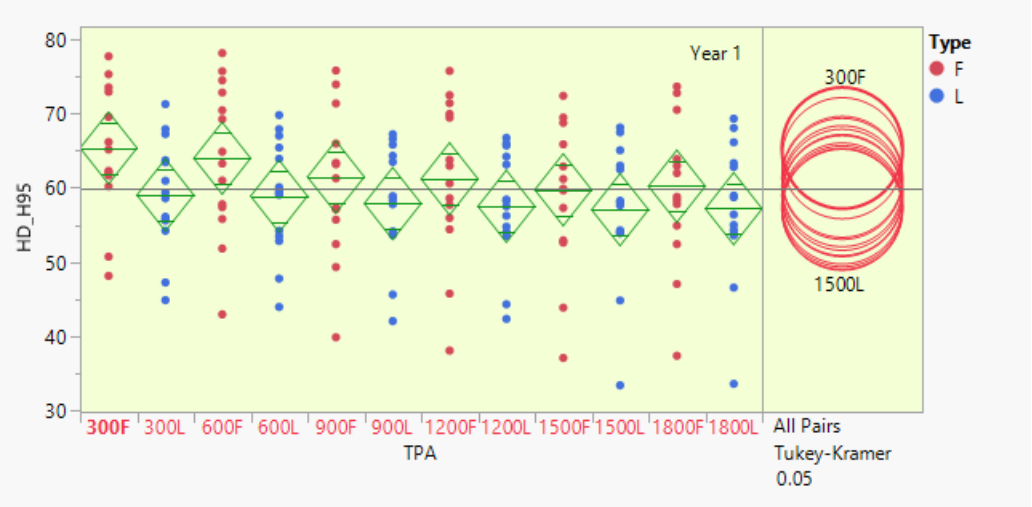

Figure 1. 10 Tukey test plot of field HD and pixel_metrics H95th percentile in ft for Year 1 by planting density. The circles in the right side denote the range of heights

Table 1.7 Tukey mean comparison of field dominant height with heights derived from pixel_metrics year 2 for all treatments or PLTPA.

Year 2												
		HD (ft)		Pixel H95TH (ft)			Pixel H99TH (ft)			Pixel Hmax (ft)		
PLTPA	N (plots)	Mean	Std Dev	Mean	Std Dev	P-Value	Mean	Std Dev	P-Value	Mean	Std Dev	P-Value
300	12	89.92	6.98	83.98	6.36		84.57	6.40		84.76	6.42	
600	14	86.63	10.03	82.34	6.88		82.92	6.93		83.10	6.94	
900	14	83.26	10.88	80.59	7.78		80.95	7.91		81.07	7.95	
1200	13	81.98	12.07	79.72	7.72	0.20	80.07	7.78	0.22	80.19	7.79	0.23
1500	12	80.94	12.10	80.27	7.94		80.59	7.99		80.68	7.99	
1800	11	80.07	12.11	79.67	8.91		79.94	8.93		80.04	8.92	

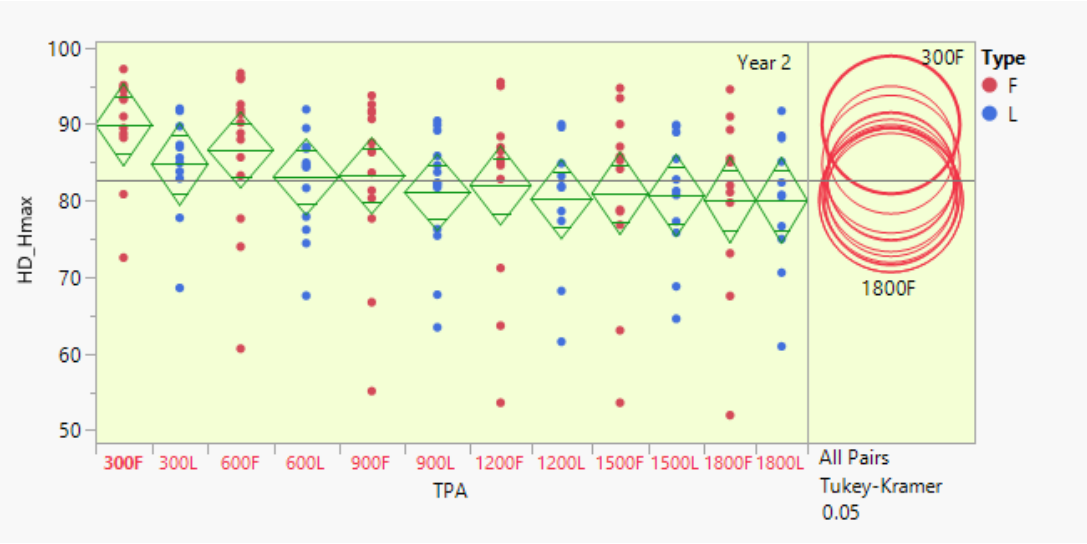

Figure 1. 11 Tukey test plot of field HD and pixel_metrics Hmax percentile in ft for Year 2 by planting density. The circles in the right side denote the range of heights

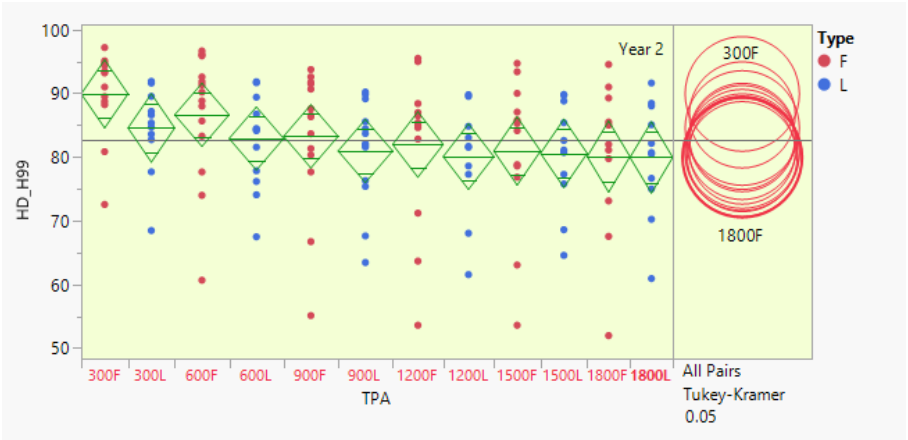

Figure 1. 12 Tukey test plot of field HD and pixel_metrics H99th percentile in ft for Year 2 by planting density. The circles in the right side denote the range of heights

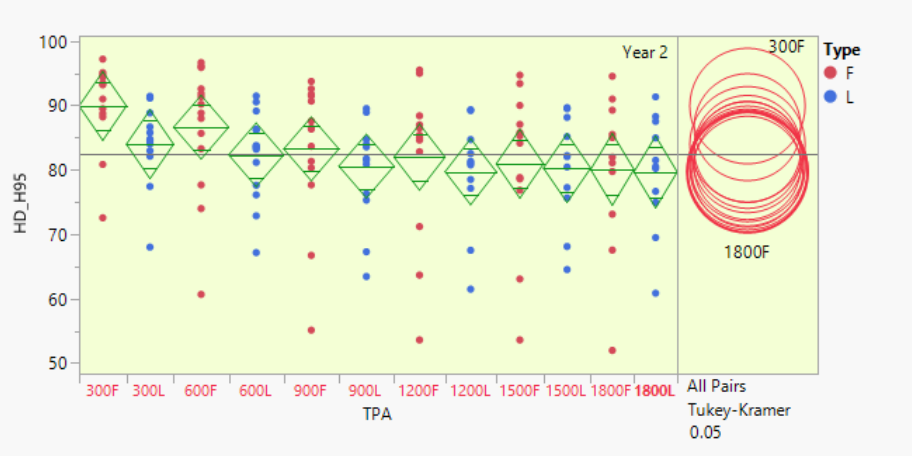

Figure 1. 13 Tukey test plot of field HD and pixel_metrics H95th percentile in ft for Year 2 by planting density. The circles in the right side denote the range of heights

Tables 1.7 and 1.8 offer a comprehensive analysis of tree height comparisons derived from field measurements (HD) and pixel_metrics, including H95TH, H99TH, and HMAX, which were extracted using the Pixel_metrics function for both Year 1 and Year 2. This pixel_metrics function from RSTUDIO combines the strengths of both Canopy Height Models (CHM) and lidar_metrics.

In Year 1 (Table 1.7), a familiar trend appears, illustrating patterns seen in previous tables. Lower PLTPA levels correlate with taller average tree heights, while higher PLTPA levels are associated with shorter mean tree heights across all three pixel_metrics: H95TH, H99TH, and HMAX. For example, at a PLTPA level of 300, the average tree height measured by HD is 65.4 ft, while the corresponding pixel metrics (H95TH, H99TH, and HMAX) yield mean heights of 59.03 ft, 59.39 ft, and 59.5 ft, respectively. Significantly, the P-values for these comparisons all exceed 0.05 (0.312, 0.4, and 0.43 for H95TH, H99TH, and HMAX, respectively), indicating a lack of statistically significant disparities between HD and pixel metrics in Year 1 across all three metrics. This underscores the statistical similarity in the estimations of tree heights provided by pixel metrics and HD, regardless of the specific metric employed.

In Year 2, a similar pattern continues. Lower PLTPA levels have higher average tree heights, while higher PLTPA levels result in lower mean tree heights for H95TH, H99TH, and HMAX. For instance, at a PLTPA level of 300, HD had a mean height of 89.92 ft, while the pixel metrics yield mean heights of 83.98 ft, 84.57 ft, and 84.76 ft for H95TH, H99TH, and HMAX, respectively. However, the P-values for these comparisons remain greater than 0.05 (0.2, 0.22, and 0.23 for H95TH, H99TH, and HMAX, respectively). This indicates that, like Year 1, there are no statistically significant differences between HD and pixel metrics in Year 2 for any of the three metrics. This suggests a continued consistency in the accuracy of pixel_metrics function in estimating tree heights compared to HD in both Year 1 and Year 2.

Bootstrapping:

We ran bootstrapping for all three methods for both Year 1 and Year 2. The results are in the table below:

Table 1.8 Results from 1000 iterations bootstrapped Tukey HSD means comparisons for field heights and CHM-derived heights and plot metrics H95th and H99th percentile for Year 1. P-values are the averaged values of all p-values from all iterations. The percentage (%) of significance shows the proportion of iterations that showed significant and non-significant p-values.

	CHM			Met_H95			Met_H99		
	P-value	not_significant (%)	significant (%)	P-value	not_significant (%)	significant (%)	P-value	not_significant (%)	significant (%)
300L-300F	0.53	87.70	12.30	0.51	87.00	13.00	0.81	98.30	1.70
600L-600F	0.62	90.90	9.10	0.64	91.70	8.30	0.85	98.40	1.60
900L-900F	0.69	93.20	6.80	0.72	94.40	5.60	0.88	99.40	0.60
1200L-1200F	0.69	93.50	6.50	0.68	92.90	7.10	0.87	98.20	1.80
1500L-1500F	0.84	98.60	1.40	0.81	97.90	2.10	0.94	99.80	0.20
1800L-1800F	0.78	97.10	2.90	0.79	96.40	3.60	0.93	99.60	0.40

Table 1.9 Results from 1000 iterations bootstrapped Tukey HSD Means comparisons for field heights and Pixel metrics H9th and H99th percentile and HMAX for Year 1. P-values are the averaged values of all p-values from all iterations. The percentage (%) of significance shows the proportion of iterations that showed significant and non-significant p-values.

	Pix_H95			Pix_H99			Pix_HMAX		
	P-value	not_significant (%)	significant (%)	P-value	not_significant (%)	significant (%)	P-value	not_significant (%)	significant (%)
300L-300F	0.86	99.10	0.90	0.86	99.10	0.90	0.86	99.20	0.80
600L-600F	0.88	99.10	0.90	0.88	99.20	0.80	0.88	99.20	0.80
900L-900F	0.91	99.60	0.40	0.91	99.60	0.40	0.91	99.60	0.40
1200L-1200F	0.92	99.50	0.50	0.92	99.50	0.50	0.92	99.50	0.50
1500L-1500F	0.95	99.80	0.20	0.95	99.80	0.20	0.95	99.80	0.20
1800L-1800F	0.94	99.70	0.30	0.94	99.70	0.30	0.94	99.70	0.30

Table 1.10 Results from 1000 iterations bootstrapped Tukey HSD means comparisons for field heights and CHM-derived heights and plot metrics H95th and H99th percentile for Year 2. P-values are the averaged values of all p-values from all iterations. The percentage (%) of significance shows the proportion of iterations that showed significant and non-significant p-values.

	CHM			Met_H95			Met_H99		
	P-value	not_significant (%)	significant (%)	P-value	not_significant (%)	significant (%)	P-value	not_significant (%)	significant (%)
300L-300F	0.49	82.00	18.00	0.69	97.30	2.70	0.94	100	0.00
600L-600F	0.73	97.10	2.90	0.72	96.20	3.80	0.93	99.8	0.20
900L-900F	0.76	97.50	2.50	0.74	96.50	3.50	0.92	99.6	0.40
1200L-1200F	0.80	96.90	3.10	0.77	95.30	4.70	0.92	99.1	0.90
1500L-1500F	0.90	98.90	1.10	0.87	98.60	1.40	0.94	99.7	0.30
1800L-1800F	0.89	99.00	1.00	0.86	98.70	1.30	0.93	99.4	0.60

Table 1.11 Results from 1000 iterations bootstrapped Tukey HSD Means comparisons for field heights and Pixel metrics H9th and H99th percentile and HMAX for Year 2. P-values are the averaged values of all p-values from all iterations. The percentage (%) of significance shows the proportion of iterations that showed significant and non-significant p-values.

	Pix_H95			Pix_H99			Pix_HMAX		
	P-value	not_significant (%)	significant (%)	P-value	not_significant (%)	significant (%)	P-value	not_significant (%)	significant (%)
300L-300F	0.77	98.9	1.1	0.82	99.4	0.6	0.84	99.7	0.3
600L-600F	0.83	98.8	1.2	0.87	99.3	0.7	0.88	99.5	0.5
900L-900F	0.9	99.2	0.8	0.91	99.6	0.4	0.92	99.4	0.6

1200L-1200F	0.9	99.1	0.9	0.92	99.4	0.6	0.92	99.4	0.6
1500L-1500F	0.94	99.6	0.4	0.94	99.7	0.3	0.95	99.6	0.4
1800L-1800F	0.93	99.3	0.7	0.93	99.3	0.7	0.93	99.1	0.9

From Tables 1.8, 1.9, 1.10, and 1.11, we observed consistent findings similar to those obtained from a single application of the Tukey test. It is noteworthy that, when employing the bootstrapping method, mean differences using the CHM were determined to be not significantly different, but it was significantly different in the Year 1 comparison. Aside from this, the overall trend remains consistent. The pixel metrics derived from the HMAX method predominantly showed non-significant differences with field height. However, in the case of the CHM method, the percentage of times being significantly different is up to 12 percent for Year 1 and 18 percent for Year 2. In contrast, this percentage is negligible for the comparison involving pixel metrics for both years.

Unmanned Aeiral Vehicle (UAV)

Mean comparison using Field Dominant Height and Canopy Height Model

Table 1. 12 Tukey mean comparison of field dominant height with heights derived from Canopy Height Model for year 3 for all treatments or PLTPA

		HD (ft)		CHM (ft)		
PLTPA	N(plot)	Mean	Std Dev	Mean	Std Dev	P-Value
300	10	94.41	4.75	76.58	6.98	0.00*
600	13	90.55	7.87	72.98	10.16	
900	13	88.65	9.32	70.02	12.07	
1200	11	86.76	9.36	69.53	13.02	
1500	12	86.45	10.23	69.58	11.14	
1800	9	84.16	9.65	66.19	14.78	

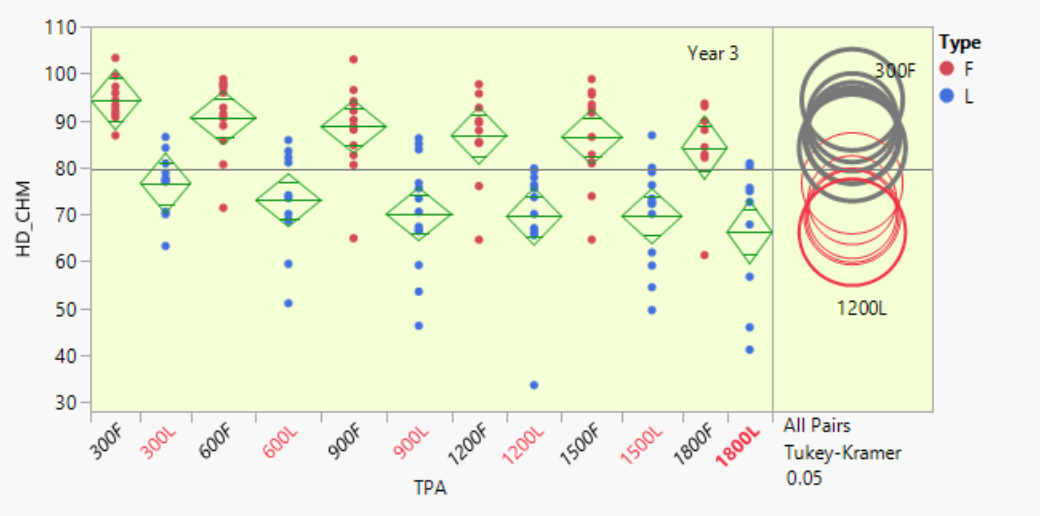

Figure 1. 14 Tukey test plot of field HD and CHM in ft for Year 3 by planting density. The circles in the right side denote the range of heights

Table 1.9 revealed significant differences in tree height measurements between field-measured dominant height (HD) and Canopy Height Model (CHM) heights obtained through UAV laser scanning for various PLTPA levels using Tukey HSD. At the lowest PLTPA level of 300, the UAV laser scanner (CHM) provided an average tree height of 76.58 ft, while the field measurements (HD) yielded a notably higher mean height of 94.41 ft. Similar trends were observed across the different PLTPA levels. As PLTPA levels increased, there was a consistent pattern of HD measurements being higher than CHM measurements. For example, at PLTPA 600, HD had a mean height of 90.55 ft compared to CHM's 72.98 ft. The trend continued with even larger differences at PLTPA 900, 1200, 1500, and 1800. The Tukey test was also found to be statistically significant with a P-value of 0.001. These findings suggest that the UAV laser scanner, even with its higher point density return, shows CHM heights tend to underestimate tree heights when compared to field measurements. This disparity indicates that CHM may have limitations in accurately estimating tree heights, especially in denser forest areas.

Mean comparison using Field_Dominant Height and lidar_metrics

Table 1. 13 Tukey mean comparison of field dominant height with heights derived lidar metrics for year 3 for all treatments or PLTPA

		HD (ft)		*Metrics H95TH (ft)*			*Metrics H99TH (ft)*		
PLTPA	N (plots)	Mean	Std Dev	Mean	Std Dev	P-Value	Mean	Std Dev	P-Value
300	10	94.41	4.75	90.39	4.12		93.53	3.90	
600	13	90.55	7.87	87.20	6.66		90	6.54	
900	13	88.65	9.32	84.84	8.60		87.67	8.53	
1200	11	86.76	9.36	85.12	5.90	0.052	88.12	5.72	0.15
1500	12	86.45	10.23	84.17	8.37		87.28	8.24	
1800	9	84.16	9.65	82.36	8.96		85.33	9.05	

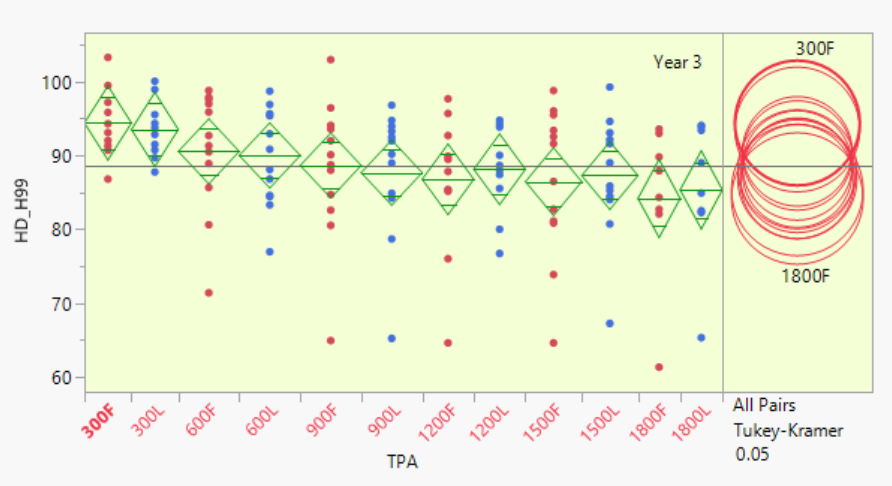

Figure 1. 15 Tukey test plot of field HD and lidar_metrics H99th percentile in ft for Year 3 by planting density. The circles in the right side denote the range of heights

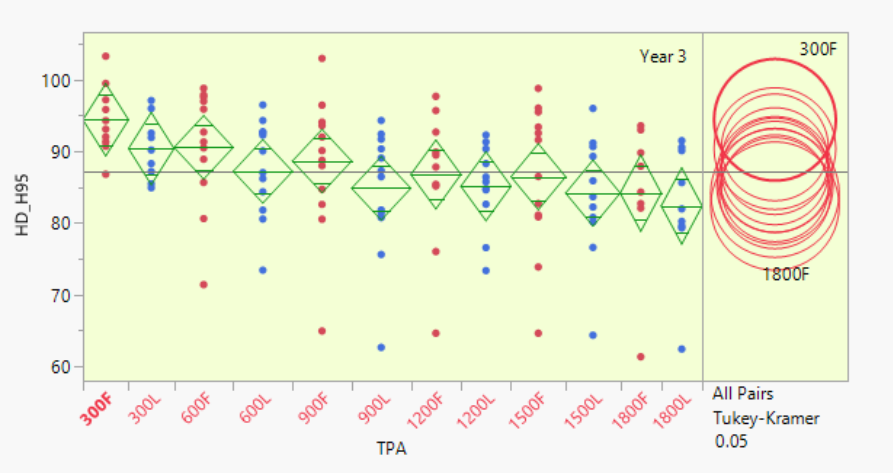

Figure 1. 16 Tukey test plot of field HD and lidar_metrics H99th percentile in ft for Year 3 by planting density. The circles in the right side denote the range of heights

Table 1.10 shows the comparison of field-measured dominant height (HD) and metrics obtained from the lidar_metrics function for various PLTPA levels. This analysis focuses on two specific metrics, H95TH and H99TH, which provide insights into different aspects of canopy height. At the lowest PLTPA level of 300, the HD measurements yielded an average tree height of 94.41 ft, with a standard deviation of 4.75. In comparison, the lidar_metrics, specifically H95TH and H99TH, produced mean heights of 90.39 ft and 93.53 ft, respectively. As the PLTPA levels increase, a similar pattern is observed, where HD measurements consistently remain slightly higher than the lidar_metrics metrics. For example, at PLTPA 600, HD records a mean height of 90.55 ft, while lidar_metrics' H95TH and H99TH metrics provide average heights of 87.2 ft and 90 ft, respectively. This trend continues through PLTPA levels of 900, 1200, 1500, and 1800, with HD consistently reporting slightly taller tree heights compared to the lidar_metrics metrics H95TH and

H99TH. The statistical analysis with P-values indicates no significant differences between HD and lidar_metrics metrics at these PLTPA levels. In essence, the data suggests that for the given PLTPA levels, the lidar_metrics H95TH and H99TH provide tree height estimations that are in close agreement with the field measurements (HD).

Mean comparison using Field_Dominant Height and pixel_metrics

Table 1. 14 Tukey mean comparison of field dominant height with heights derived pixel metrics for year 3 for all treatments or PLTPA

		HD (ft)		*Pixel H95TH (ft)*			*Pixel H99TH (ft)*			*Pixel Hmax (ft)*		
PLTPA	N (plots)	Mean	Std	Mean	Std Dev	P-Value	Mean	Std Dev	P-Value	Mean	Std Dev	P-value
300	10	94.41	4.75	92.25	4.06		94.41	4.75		91.97	3.73	
600	13	90.55	7.87	88.89	6.46		90.56	7.87		89.17	5.79	
900	13	88.65	9.32	86.49	8.7		88.64	9.33		87.93	8.59	
1200	11	86.76	9.36	86.82	6.2	0.12	86.76	9.36	0.12	90.19	4.64	0.3
1500	12	86.45	10.23	85.85	8.3		86.45	10.23		88.62	7.46	
1800	9	84.16	9.65	83.83	8.99		84.16	9.65		86.56	9.72	

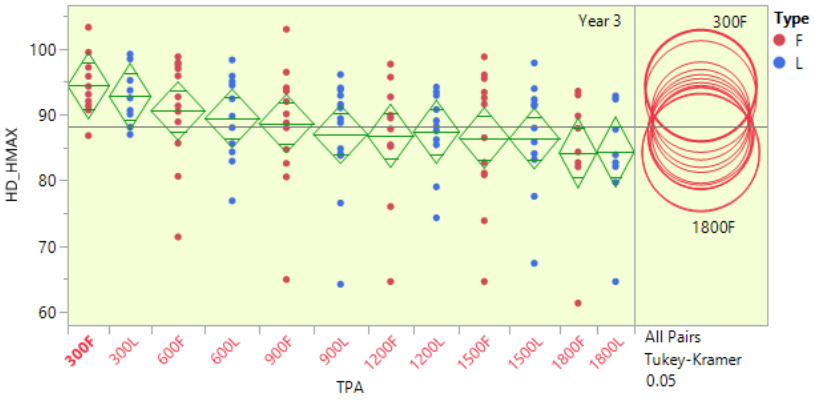

Figure 1. 17 Tukey test plot of field HD and pixel_metrics Hmax percentile in ft for Year 3 by planting density. The circles in the right side denote the range of heights

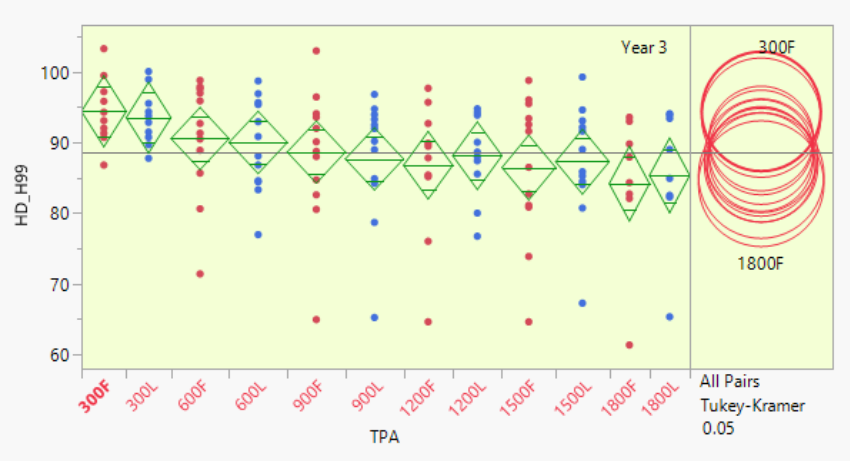

Figure 1. 18 Tukey test plot of field HD and pixel_metrics H99th percentile in ft for Year 3 by planting density. The circles in the right side denote the range of heights

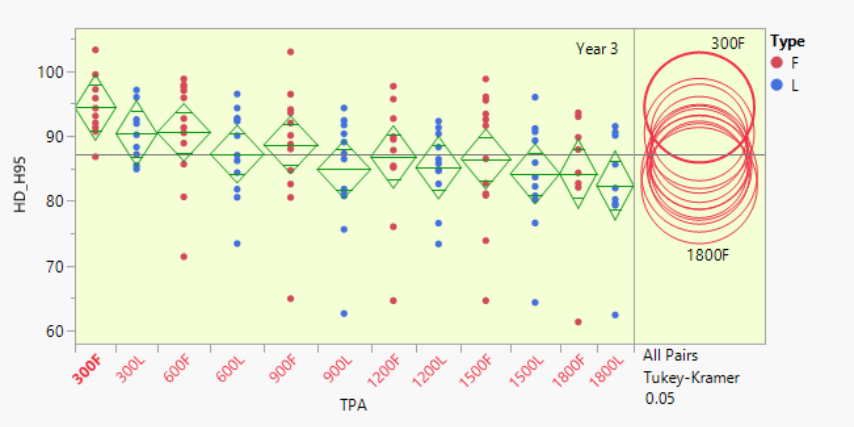

Figure 1. 19 Tukey test plot of field HD and pixel_metrics H95th percentile in ft for Year 3 by planting density. The circles in the right side denote the range of heights

Similar to ALS, UAV pixel metrics also generated negligible mean differences in lidar height comparison to HD. It became evident that with increasing point density from Unmanned Aerial Vehicle (UAV) data, there was a reduced tendency to underestimate lidar heights compared

to ALS, which features a lower point density. For example, at PLTPA 1200, HD records an average height of 86.76 ft, while pixel metrics reveal mean heights of 86.82 ft for H95TH, 86.76 ft for H99TH, and 90.19 ft for Hmax. It also has a similar pattern that height reduces as increasing trees per plot density. Furthermore, the Tukey test consistently establishes the absence of statistically significant differences between HD and pixel metrics across all metrics and various PLTPA levels.

Bootstrapping:

The bootstrapping of Tukey HSD for UAV LiDAR and Field dominant height also showed similar results. Table below shows following results:

Table 1.15 Results from 1000 iterations bootstrapped Tukey HSD Means comparisons for field heights and UAV-derived CHM metrics and H9th and H99th percentile plot metrics for Year 3. P-values are the averaged values of all p-values from all iterations. The percentage (%) of significance shows the proportion of iterations that showed significant and non-significant p-values.

	CHM			Met_H95			Met_H99		
PLTPA	P-value	not_significant (%)	significant (%)	P-value	not_significant (%)	significant (%)	P-value	not_significant (%)	significant (%)
300L-300F	0.05	22.30	77.70	0.95	100.00	0.00	1.00	100.00	0.00
600L-600F	0.03	13.00	87.00	0.93	99.90	0.10	0.97	100.00	0.00
900L-900F	0.03	9.30	90.70	0.79	96.60	3.40	0.93	99.50	0.50
1200L-1200F	0.09	26.80	73.20	0.94	99.80	0.20	0.95	99.30	0.70
1500L-1500F	0.09	25.80	74.20	0.88	97.60	2.40	0.92	99.10	0.90
1800L-1800F	0.16	37.20	62.80	0.91	98.80	1.20	0.92	99.30	0.70

Table 1.16 Results from 1000 iterations bootstrapped Tukey HSD Means comparisons for field heights and UAV-derived Pixel metrics H9th and H99th percentile and HMAX for Year 3. P-values are the averaged values of all p-values from all iterations. The percentage (%) of significance shows the proportion of iterations that showed significant and non-significant p-values.

	Pix_H95			Pix_H99			Pix_HMAX		
PLTPA	P-value	not_significant (%)	significant (%)	P-value	not_significant (%)	significant (%)	P-value	not_significant (%)	significant (%)
300L-300F	1.00	100.00	0.00	1.00	100.00	0.00	1.00	100.00	0.00
600L-600F	0.98	100.00	0.00	0.97	100.00	0.00	0.97	99.90	0.10

900L-900F	0.93	99.20	0.80	0.92	99.20	0.80	0.91	99.10	0.90
1200L-1200F	0.83	97.50	2.50	0.81	96.80	3.20	0.78	96.40	3.60
1500L-1500F	0.86	97.80	2.20	0.85	97.50	2.50	0.84	97.40	2.60
1800L-1800F	0.82	96.60	3.40	0.81	96.00	4.00	0.80	95.50	4.50

CHM method was highly significant in the Tukey comparison, and it is significant in bootstrapping as well. The p-values across different TPA are significantly different for less dense trees and they are slightly non-significantly different for high density TPA plots. The percentage of non-significant differences ranges from 9 to 38 percent. However, using pixel_metrics Hmax, p-values are not significant in each mean comparison and have very less percentage of significant differences.

5. DISCUSSION AND CONCLUSION:

In this study, we conducted an analysis where we extracted LiDAR tree heights using different methods and compared them with the dominant heights obtained from field measurements. The three methods used, namely CHM, lidar_metrics, and pixel_metrics, showed no significant differences when compared to the field-based dominant heights. Nevertheless, there were variations in how effectively and to what extent LiDAR heights from one method compared to another differed from the field measurements.

The CHM method demonstrated non significant differences only when compared with LiDAR data with high point densities, such as data from a later year of Airborne Laser Scanning (ALS) and UAV point cloud. This occurs because a CHM is constructed using algorithms to estimate canopy height. When the point density is insufficient, CHM typically yields height results that are underestimated compared to the field-derived dominant heights. Nelson et al. (2010) observed that the CHM derived from a low point density LAS data in permanent plots tended to underestimate canopy height, resulting in an overestimation of biomass. Nevertheless, a high-resolution CHM still holds potential for advanced modeling of forest attributes and eventual applications in forest modeling, including climate modeling and biomass estimation. (Cao et al., 2016; De Frenne et al., 2019).

The second approach for extracting tree height involved the utilization of lidar metrics, a method based on extracting a variety of height-related metrics, including mean, median, maximum, percentile heights, and density metrics, directly from point clouds (Popescu & Zhao, 2008). This method employs a single height return for height extraction per plot, meaning it considers only one value representing the height for a specific percentile, such as the 95th percentile, from the entire plot's point cloud. Our analysis of the results revealed that dominant

heights (HD) exhibited nonsignificant differences when compared to the lidar metrics 99th percentile height for both ALS and UAV-lidar data. An interesting finding emerged in the context of ALS, where H95th was significantly different from HD. However, with the UAV-lidar data having higher resolution compared to ALS, there was no significant difference between HD from the field and the H95th mean value. This observation suggests that the point density or resolution of LiDAR data plays a crucial role in accurately estimating the dominant height of trees. Numerous other studies have also suggested that low point density LiDAR data leads to decreased accuracy and tends to underestimate tree heights. Moreover, it results in less clear detection of tree canopy shape, thereby affecting the accuracy and comparability of height extraction with field-measured dominant height (Kwak et al., 2007; Matti Maltamo, 2014; Nelson, 1997). Therefore, lack of required point density from the ground structure does effect the accuracy of estimation from LiDAR (Popescu, Wynne, & Nelson, 2002; Thomas et al., 2006). However, a relatively low density lidar point spacing can still offer reliable accuracy in plot level height estimation. Tesfamichael, Ahmed and Van Aardt (2010) found similar result in eucalyptus plantation. For instance, Heurich et al. (2004) reported tree height estimations with an accuracy of 0.96 and 0.98 for deciduous and coniferous trees, respectively, when using a point density of 10 points m^{-2}.

The pixel_metrics method, generating mean values from raster layers for maximum, 95^{th}, and 99^{th} metrics at 5 m for ALS and 1 m for UAV pixel resolution, allowed us to preserve the variability of tree heights, in contrast to the lidar_metrics method, which considers only a single return for metric extraction. Previous studies have recognized the advantages of LiDAR-derived grid or pixel data, highlighting their compact storage, expedited data processing, and utility for direct tree measurements (Brandtberg, 2003; Maltamo et al., 2004; Popescu, Wynne, & Nelson,

2002). But they were using CHM, a method that has its own set of challenges, including issues related to data pits and the quality of tree crowns, which can lead to an underestimation of tree heights. Interestingly, our results confirm this underestimation issue in CHM. However, when comparing the tree heights derived from the pixel_metrics method with the field-measured dominant height (HD), we observed no significant differences over all three years, regardless of point density. Furthermore, it is worth noting that even the heights corresponding to the 95th percentile exhibited no discernible difference from HD. In contrast, Hmax consistently demonstrated a closer resemblance to HD. This alignment may be attributed to the pixel_metrics method's capacity to retain the variability in tree heights. Simultaneously, by applying the 95th percentile return filter, we effectively extracted heights from the largest trees, akin to the definition of dominant height in the PMRC HD definition, which considers the dominant height as the average height of trees exceeding the mean diameter.

In summary, our study highlights the significance of LiDAR data resolution, emphasizing that higher point density is essential for accurate tree height estimations. The pixel_metrics method, with its ability to retain height variability and extract heights from the largest trees, offers promising prospects for precise forest inventory and modeling. These findings contribute to the growing body of knowledge surrounding LiDAR technology's applications in forestry and its potential for enhanced accuracy in forest attribute estimation.

6. REFERENCES

- Ashton, P. S., & Liu, J. (1995). Individual-based simulation models for forest succession and management. *Forest Ecology & Management*, *73*(1-3), 157. https://doi.org/10.1016/0378-1127(94)03490-N
- Avery, T. E., & Burkhart, H. E. (2015). *Forest Measurements*. Waveland Press, Incorporated. https://books.google.com/books?id=_T1ArgEACAAJ
- Bettinger, P., Boston, K., Siry, J. P., & Grebner, D. L. (2016). *Forest management and planning*. Academic press.
- Buchman, R. G., & Shifley, S. R. (1983). Guide to Evaluating Forest Growth Projection Systems. *Journal of Forestry*, *81*(4), 232-254. https://doi.org/10.1093/jof/81.4.232
- Burkhart, H., & Tomé, M. (2012). *Modeling Forest Trees and Stands*. https://doi.org/10.1007/978-90-481-3170-9
- Burt, A., Disney, M., Calders, K., & Goslee, S. (2018). Extracting individual trees from lidar point clouds using
- treeseg. *Methods in Ecology and Evolution*. https://doi.org/10.1111/2041-210x.13121
- Cao, L., Coops, N. C., Innes, J. L., Sheppard, S. R. J., Fu, L., Ruan, H., & She, G. (2016). Estimation of forest biomass dynamics in subtropical forests using multi-temporal airborne LiDAR data. *Remote Sensing of Environment*, *178*, 158-171. https://doi.org/10.1016/j.rse.2016.03.012
- Chapman, H. H., & Meyer, W. H. (1949). *Forest Mensuration*. McGraw-Hill. https://books.google.com/books?id=1uosAQAAMAAJ
- Chave, J., Rejou-Mechain, M., Burquez, A., Chidumayo, E., Colgan, M. S., Delitti, W. B., Duque, A., Eid, T., Fearnside, P. M., Goodman, R. C., Henry, M., Martinez-Yrizar, A., Mugasha, W. A., Muller-Landau, H. C., Mencuccini, M., Nelson, B. W., Ngomanda, A., Nogueira, E. M., Ortiz-Malavassi, E., . . . Vieilledent, G. (2014). Improved allometric models to estimate the aboveground biomass of tropical trees. *Glob Chang Biol*, *20*(10), 3177-3190. https://doi.org/10.1111/gcb.12629
- Clutter, J. L., & Jones, E. P. (1980). *Prediction of growth after thinning in old-field slash pine plantations* (Vol. 217). Department of Agriculture, Forest Service, Southeastern Forest Experiment ….
- Eugene, A. T., & E., B. H. (1983). Forest measurements. 3rd ed.
- Harrison, W. M., & Borders, B. E. (1996). Yield prediction and growth projection for site-prepared loblolly pine plantations in the Carolinas, Georgia, Alabama, and Florida. https://doi.org/http://pmrc.uga.edu/TR1996-1.pdf
- Haynes, R. W. (2003). *An analysis of the timber situation in the United States: 1952 to 2050* (Vol. 560). US Department of Agriculture, Forest Service, Pacific Northwest Research Station.
- Maggi, K., Qinghua, G., Wenkai, L., & Marek, K. J. (2013). Delineating Individual Trees from Lidar Data: A Comparison of Vector- and Raster-based Segmentation Approaches [article]. *Remote Sensing*, *5*(9), 4163-4186. https://doi.org/10.3390/rs5094163
- Munro, D. D. (1974). Forest growth models-a prognosis. In *Growth models for tree and stand simulation* (Vol. 30, pp. 7-21). Research Note 30. Department of Forest Yield Research, Royal College of ….

- Nepal, S. K., & Somers, G. L. (1992). A generalized approach to stand table projection. *Forest science*, *38*(1), 120-133.
- Pienaar, L. V., & Harrison, W. M. (1989). A STAND TABLE PROJECTION APPROACH TO YIELD PREDICTION IN UNTHINNED, EVEN-AGED STANDS[1]. Proceedings of the Fifth Biennial Southern Silvicultural Research Conference: Memphis, Tennessee, November 1-3, 1988,
- Pretzsch, H. (2010). *Forest Dynamics, growth and yield from measurement to model*. Springer. https://doi.org/https://doi.org/10.1007/978-3-540-88307-4
- Puettmann, K. J., Wilson, S. M., Baker, S. C., Donoso, P. J., Drössler, L., Amente, G., Harvey, B. D., Knoke, T., Lu, Y., & Nocentini, S. (2015). Silvicultural alternatives to conventional even-aged forest management-what limits global adoption? *Forest Ecosystems*, *2*(1), 1-16.
- Robinson, A. P., & Monserud, R. A. (2003). Criteria for comparing the adaptability of forest growth models [Article]. *Forest Ecology and Management*, *172*(1), 53-67. https://doi.org/10.1016/S0378-1127(02)00041-5
- Roise, J. P., Harnish, K., Mohan, M., Scolforo, H., Chung, J., Kanieski, B., Catts, G. P., McCarter, J. B., Posse, J., & Shen, T. (2016). Valuation and production possibilities on a working forest using multi-objective programming, Woodstock, timber NPV, and carbon storage and sequestration. *Scandinavian Journal of Forest Research*, *31*(7), 674-680. https://doi.org/10.1080/02827581.2016.1220617
- Samuelson, P. A. (1976). Economics of Forestry in an Evolving Society. *Economic Inquiry*, *14*(4), 466-492. https://doi.org/10.1111/j.1465-7295.1976.tb00437.x
- Silva, C., Klauberg, C., Hudak, A., Vierling, L., Jaafar, W., Mohan, M., Garcia, M., Ferraz, A., Cardil, A., & Saatchi, S. (2017). Predicting Stem Total and Assortment Volumes in an Industrial Pinus taeda L. Forest Plantation Using Airborne Laser Scanning Data and Random Forest. *Forests*, *8*(7). https://doi.org/10.3390/f8070254
- Torresan, C., Berton, A., Carotenuto, F., Di Gennaro, S. F., Gioli, B., Matese, A., Miglietta, F., Vagnoli, C., Zaldei, A., & Wallace, L. (2017). Forestry applications of UAVs in Europe: A review. *International Journal of Remote Sensing*, *38*(8-10), 2427-2447.
- Wallace, L., Lucieer, A., Watson, C., & Turner, D. (2012). Development of a UAV-LiDAR System with Application to Forest Inventory. *Remote Sensing*, *4*(6), 1519-1543. https://doi.org/10.3390/rs4061519
- Weiskittel, A. R. (2011). *Forest growth and yield modeling* [Bibliographies
- Non-fiction]. Wiley. https://search.ebscohost.com/login.aspx?direct=true&AuthType=ip,shib&db=cat06564a&AN=uga.9939510163902959&site=eds-live&custid=uga1
- Wulder, M. A., White, J. C., Nelson, R. F., Næsset, E., Ørka, H. O., Coops, N. C., Hilker, T., Bater, C. W., & Gobakken, T. (2012). Lidar sampling for large-area forest characterization: A review. *Remote Sensing of Environment*, *121*, 196-209. https://doi.org/https://doi.org/10.1016/j.rse.2012.02.001
- Yang, S.-I., & Burkhart, H. E. (2020). Evaluation of total tree height subsampling strategies for estimating volume in loblolly pine plantations. *Forest Ecology and Management*, *461*. https://doi.org/10.1016/j.foreco.2020.117878

CHAPTER 2

ENHANCING YIELD PROJECTION MODELS THROUGH THE INTEGRATION OF OPTIMAL LIDAR-DERIVED MULTI-TEMPORAL HEIGHTS

1. BACKGROUND:

Effective forest management demands a comprehensive understanding of the complex dynamics of forest growth. The capacity to make informed decisions, whether they are significant primary strategies or small specific decisions, site-specific choices, centers upon this understanding. To achieve a harmonious balance between ecological, economic, and social objectives, a forest manager must possess a profound understanding of forest mensuration, silviculture, and business concepts (Bettinger et al., 2016). To better unite these factors, a forest manager should formulate a comprehensive plan that aligns with the forest requirements and objectives. Such a plan should include guidelines for executing activities, forecasting future growth, harvesting schedules, and optimizing resource utilization. If the management plan is lacking or too short-term, it can lead to unexpected issues that may impact the landowner's profits (Puettmann et al., 2015). To make a long term management plan, forest current conditions information must be needed. For this, Forest inventory is the most critical tool. Forest inventory is critical for forest plantation managers to support decisions such as forest cover, growth, yield, land attributes and resource allocation of their plantations (Roise et al., 2016; Silva et al., 2017a; Wulder et al., 2012). Forest inventory encompasses a range of data, including details about trees like their species, size (diameter and height), crown condition, and any defects. It also involves information about the site, such as soil type, moisture levels, temperature, and elevation.

Additionally, it covers aspects related to land use and land cover in the forest. As forest inventory attributes are dynamic and changing continuously, it is important to project tree attributes ahead of time to support forest managers in planning required silvicultural decisions for forest management (Eugene & E., 1983). Simulation models on computers for growth and yield offer foresters the ability to project and predict the future growth and conditions of a forest, enabling them to plan accordingly. Samuelson (1976) stressed the significance of understanding future yields, which is crucial for assessing economic aspects like future lumber prices, input costs such as planting, fertilization, thinning, pruning, and taxation within the forestry. Timberland acquisitions heavily rely on and can be impacted by growth and yield projection equations, as these equations are utilized to estimate future timber harvesting plans (Haynes, 2003).

Forest growth modeling is a holistic process that involves a deep understanding of the current forest conditions, data collection for modeling, and the pursuit of improvements to existing models. Several models have been developed to address forestry related challenges at various spatial and temporal scales, including individual tree, size class, stand, and landscape levels (Pretzsch, 2010). For example, individual tree growth and yield models enable the stratification of each tree, projecting their growth, determining optimal harvest times and quantities. Additionally, there are models designed for assessing stand dynamics at the stand level, such as evaluating site-specific silvicultural systems. Hence, numerous models are available to forest managers, providing them with the capability to forecast and project in alignment with their specific requirements (Ashton & Liu, 1995) and over time, there has been a continual development of new models aimed at enhancing the accuracy of existing models and integrating new components in response to technological advancements in forestry, as well as to meet current forest landowners demands (Chave et al., 2014). With availability of several models, it can be a challenge for managers to

select and evaluate which model should be ideal to use for their forest management (Buchman & Shifley, 1983). Nonetheless, among the many models available, it is impossible to validate or determine that any model is the best representation of the reality(Robinson & Monserud, 2003). Hence, the good model depends upon the application and operational needs of the forest manager and in which type of forest they are working on. There are several publications offering a whole explanation of steps and things to be considered before choosing a growth and yield model (Buchman & Shifley, 1983; Burkhart & Tomé, 2012; Weiskittel, 2011).

Loblolly pine, being one of the most extensively planted species in the southeastern United States, has led to the development of numerous existing forest growth and yield projection models. For stand level, growth model started with a common simple assumption on diameter growth and mortality (Chapman & Meyer, 1949; Eugene & E., 1983). Clutter and Jones (1980) and Pienaar and Harrison (1989) developed growth and mortality equations, with the assumption that relative tree size could be a tool to assess stand-mortality, and relative tree size mostly are constant over time. Later, a method was found in which trees in each class were assumed to follow a Weibull distribution (Nepal & Somers, 1992). Cao et al. (2016) incorporated these methods to project a stand table which predicts the mortality as well as diameter growth for each of the diameter class trees with use of individual tree model. Individual tree models are categorized into two main classes: distance-independent and distance-dependent models. This categorization is based on whether the models require information about the locations of individual trees.

Individual-tree models can be categorized into two distinct classes: distance-independent and distance-dependent models. This categorization depends on whether the models require information about the locations of individual trees (Munro, 1974). Distance independent models project the growth of trees, either on an individual basis or by size classes, primarily as a function

of their current size and stand-level variables, such as age, site quality, and basal area per unit area. Typically, these models consist of three essential components: (1) a component for predicting diameter growth; (2) a component for predicting height growth (or a height/diameter relationship used to estimate tree heights from diameter at breast height values); and (3) a component for modeling tree mortality. Finally, to determine growth and yield, foresters use their individual tree volume or weight functions on the data of their simulated tree heights and basal area.

Unfortunately, height growth projection is affected by the level of bias in the method of measuring tree height in the field and the diameter function used to calculate height at stand level. Numerous researchers have reported instances where foresters frequently resort to imprecise, unreliable, and biased estimates, resulting in elevated measurement errors within growth and yield models that incorporate tree height as a predictive factor in their growth equations (Avery & Burkhart, 2015; Yang & Burkhart, 2020).

The purpose of this research was to assess and compare the projected tree heights, volume and weight derived from field measurements with those obtained through LiDAR-based projections using the PMRC 1996 projection model (Harrison & Borders, 1996) in loblolly pine plantations. This comparison was conducted across seven PMRC loblolly pine research sites: four within the Coastal Plain Culture Density (CPCD) study and three falling under the South Atlantic Gulf Slope Studies (SAGSCD). The PMRC model is utilized by various members of the research cooperative, including timberland companies, private forest landowners, and researchers, to quantify their plantation resources. Given the prevalence of loblolly pine plantations as a dominant softwood species in the southeastern United States, comparing optimal tree height projections in these equations holds value for forest managers aiming to model yield and maximize their plantation returns.

2. OBJECTIVES:

- To assess the differences between LiDAR-projected tree heights from year 1 to year 2 and the actual dominant heights observed in the field.
- To evaluate the accuracy of yield predictions derived from both field-projected heights and LiDAR-projected heights from year 1 to year 2 in comparison to the actual yields recorded in year 2.

3. METHOD:

Field Data:

In this study, data for dominant height projection was collected from seven installations of CPCD and SAGSCD located across the states of Alabama, Georgia, South Carolina, and Florida. Each installation comprised 12 plots, each with a planting density of 300, 600, 900, 1200, 1500, and 1800 trees per acre. It's worth noting that some plots experienced tree mortality, leading to the absence of data in later years. All plots are located in the Upper Coastal Plain region.

To make our projection, we used two different sets of data. The first set is from the early years, known as year 1, and the second set is for the year we want to project to, which we called as year 2. We selected these years based on the free USGS LiDAR data available from previous installations. The plantation age range of the plot data for the first year ranged from 12 to 17 years. This data was projected to an age range of 21 to 24 years using Equation (1). Dominant trees were identified based on the PMRC height definition, which classified trees with a Diameter at Breast Height (DBH) greater than the arithmetic mean for each age interval. Trees with recorded DBH and height measurements were included in the dominant height calculation, while those with missing data were excluded. Once the projected heights were determined, we calculated yield in

terms of Total Volume Over Bark (TVOB) and Green Weight Over Bark (GWOB) using actual Basal Area (BA) and Trees per Acre (TPA) for each year, as described by the PMRC equations (Harrison & Borders, 1996) below:

$$HD_2 = HD_1 \left[\frac{1-e^{-0.014452*A_2}}{1-e^{-0.014452*A_1}}\right]^{0.8216} \quad (1)$$

$$\ln(Y) = b_0 + b_1 \ln(HD) + b_2 \ln(BA) + b_3 \frac{\ln(TPA)}{A} + b_4 \frac{\ln(HD)}{A} + b_5 \frac{\ln(BA)}{A} \quad (2)$$

Where, Equation (1), HD2 represents the projected height from age A1 to age A2. In Equation (2), Y denotes the yield per acre for TVOB and GWOB, where BA stands for basal area, TPA represents trees per acre, and projected HD is the dominant height for that year. Parameter estimates for the Yield equation are provided in Table 1.

Table 2. 1 Parameter estimates for Yield equation with respective TVOB and GWOB

Yield	b_0	b_1	b_2	b_3	b_4	b_5
TVOB	0	0.268552	1.368844	-7.46686	8.934524	3.553411
GWOB	-3.81802	0.430179	1.276768	-8.08879	7.428472	5.554509

LiDAR data:

For the LiDAR data, heights were extracted using the optimal method, which involved utilizing the maximum height (HMAX) from the pixel_metrics method for the initial year. This initial year data corresponded to the same age range as the actual field dominant heights (12-17 years). A detailed explanation of the height extraction method is provided in Chapter 1. After obtaining the initial year LiDAR heights, Equation (1) was applied to project these heights to the

second year age range (21 to 24 years). Following the same procedure as in the field data, yield calculations for the second year were performed using Equation (2).

Statistical Analysis:

Comparison of Projected Height Means:

We performed a comparative analysis between the actual field HD and LiDAR-derived heights, considering the specific year of projection. The Tukey Honest Significant Difference (HSD) test in the R software was utilized for this purpose, enabling us to discern whether the projected LiDAR heights significantly deviated from the actual HD for that particular year. In this process, we established a 95 percent confidence interval by considering both the lower and upper bounds for a rigorous assessment of mean differences.

Comparison of Predicted Yields:

We conducted an in-depth assessment of the calculated Yield, encompassing both Total Volume Over Bark (TVOB) and Green Weight Over Bark (GWOB), by employing a linear regression analysis. The primary objective of this analysis was to examine the statistical relationship between the predicted yield and the actual yield. The goal was to quantify the degree to which the predicted values align with the observed values, offering valuable insights into the precision of our predictive model. The regression model employed treated the actual yield as the dependent variable, as our primary interest was in understanding how it is influenced by the predicted yield. The regression equation used was expressed as follows:

$$Actual\ Yield\ =\ \beta 0\ +\ \beta 1\ \times\ Predicted\ Yield\ +\ \varepsilon \quad (2)$$

Where, β0 represents the intercept, β1 the slope, and ε signifying the error term encompassing unexplained variation.

To evaluate the performance of the regression, we used the coefficient of determination (R^2), Mean Bias Error (MBE), and Root Mean Square Error (RMSE).

a. Coefficient of Determination (R-squared, R^2):

R-squared measures the fraction of the variability in the dependent variable accounted for by the independent variables within a regression model.

$$R^2 = 1 - \frac{SSR}{SST} \quad (3)$$

Where, SSR (Sum of Squared Residuals) represents the sum of the squared disparities between the actual yield and the predicted yield, while SST (Total Sum of Squares) denotes the sum of the squared deviations between the actual values and the mean of the actual values.

b. Mean Bias Error (MBE):

MBE is defined as the average difference between the actual and predicted values. It helps assess whether the model tends to overestimate or underestimate the actual values.

$$MBE = \frac{1}{n}\sum_{i=1} n\ (Actual_i - Predicted_i) \quad (4)$$

c. Root Mean Square Error (RMSE):

RMSE is a measure of the average magnitude of the errors between actual and predicted values. A lower RMSE indicates a better fit of the model to the data.

$$RMSE = \sqrt{\frac{1}{n}\sum_{i=1} n\,(Actual_i - Predicted_i)^2} \quad (5)$$

d. MAPE (Mean Absolute Percent Error):

MAPE is the average percentage difference between predicted values and actual values. It quantifies the accuracy of predictions in terms of percentage errors.

$$MAPE = \frac{1}{n}|\sum_{i=1} n\ (Actual_i - Predicted_i)| * 100 \quad (6)$$

Where in equation 4, 5, and 6, n is total number of observations, and $Actual_i$ represents actual yield, $Predicted_i$ represents the predicted yield.

4. RESULTS:

Mean comparison of Projected Field HD with projected LiDAR Hmax:

We have compared two distinct methods of projecting tree height: Field Projected HD (Dominant Height) and LiDAR Projected Hmax (LiDAR-derived height data). This evaluation was performed across a range of planting densities (PLTPA). The analysis of the results has unveiled noteworthy trends that provide essential insights into the performance and characteristics of these two height projection methods.

Table 2. 2 Summary statistics with Tukey HSD from the Field and LiDAR projected heights from year 1 (age 12-17) to year 2 (age 21-24)

	Actual HD (ft)				Projected LiDAR Hmax (ft)				Tukey HSD
PLTPA	Mean	SD	Min	Max	Mean	SD	Min	Max	P-value
300	90.50	5.64	79.00	97.20	85.94	6.22	70.98	92.34	0.08
600	87.50	8.38	66.26	96.67	83.93	7.42	71.87	91.94	
900	84.10	9.08	61.50	93.75	81.71	8.68	63.08	91.19	
1200	84.00	9.78	59.77	95.50	82.29	6.65	71.57	91.47	
1500	82.10	9.85	60.55	94.71	79.84	8.54	59.28	91.01	
1800	80.90	10.58	56.88	94.54	80.24	9.33	60.03	91.54	

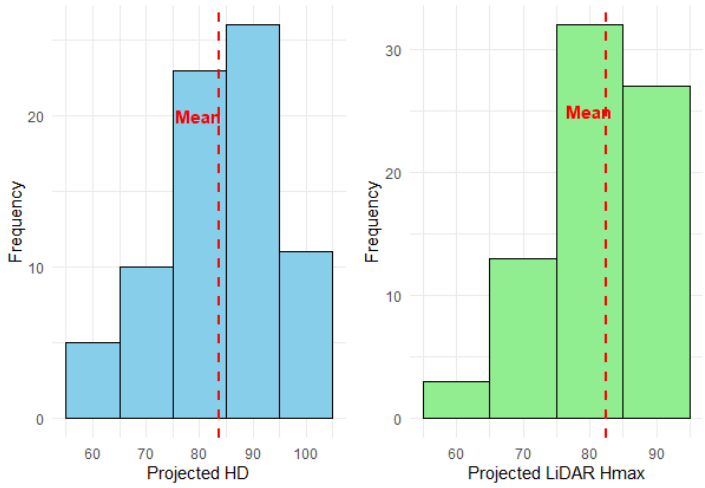

Figure 2. 1 Histograms of projected HD from the Field observation on the left and Projected LiDAR Hmax on the right. Both histograms illustrate that the heights are normally distributed.

From table 2.2, we observed that the Field Projected HD method consistently produces higher mean height values when compared to the LiDAR Projected Hmax method, regardless of the planting density. This discrepancy suggests that the Field Projected HD method tends to overestimate tree heights in contrast to the LiDAR method. Additionally, the Field Projected HD method exhibits slightly higher standard deviation values, indicating greater variability in the field-projected heights. On the other hand, both methods effectively capture the tallest trees, as evidenced by similar maximum values. However, the LiDAR Projected Hmax method seems to provide more consistent height estimates for shorter trees, as reflected in the minimum values.

Mean comparison of Actual Field HD with projected LiDAR Hmax:

Table 2.3 provides a comprehensive overview of Actual HD and Projected LiDAR Hmax values across various categories of PLTPA. Notable trends can be seen from the data. In several instances, the mean values of Actual HD surpass those of Projected LiDAR Hmax. For instance, at the PLTPA 300 level, the mean of Actual HD is 90.45 ft, while Projected LiDAR Hmax averages 85.94 ft. These observations indicate that, on average, Actual HD values tend to be higher than those of Projected LiDAR Hmax. Regarding statistical significance, the presence of a Tukey HSD p-value of 0.08 suggests a lack of significant difference between Actual HD and Projected LiDAR Hmax.

Table 2. 3 Comparison of Actual HD and Projected LiDAR Hmax across PLTPA levels with Tukey HSD Analysis

	Actual HD (ft)				Projected LiDAR Hmax (ft)				Tukey HSD
PLTPA	Mean	SD	Min	Max	Mean	SD	Min	Max	P-value
300	90.45	5.64	79.00	97.20	85.94	6.22	70.98	92.34	0.08
600	87.51	8.38	66.26	96.67	83.93	7.42	71.87	91.94	
900	84.07	9.08	61.50	93.75	81.71	8.68	63.08	91.19	
1200	84.02	9.78	59.77	95.50	82.29	6.65	71.57	91.47	
1500	82.09	9.85	60.55	94.71	79.84	8.54	59.28	91.01	
1800	80.90	10.58	56.88	94.54	80.24	9.33	60.03	91.54	

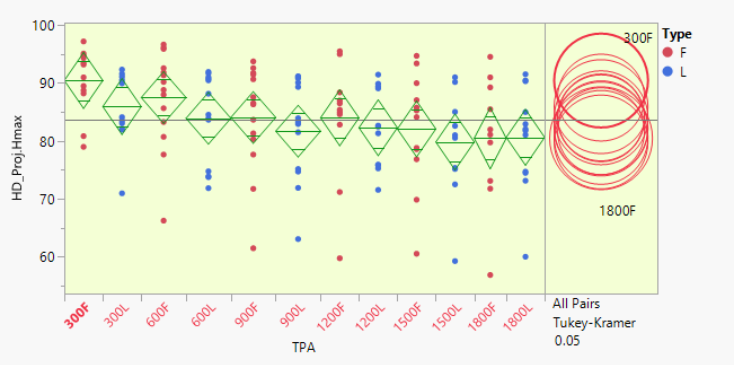

Figure 2. 2 Tukey test between projected LiDAR Hmax height and actual height in ft at year 2

Model comparison for tree volume:

Table 2.4 presents a summary of the linear regression equations generated by using Field-projected Total Volume Over Bark (TVOB) and LiDAR-projected TVOB against the actual TVOB at Year 2. The table presents key metrics that help us understand the quality of these regression models and their ability to predict actual TVOB accurately.

Table 2. 4 Summary of Linear regression between Field projected TVOB and LiDAR projected TVOB with Actual TVOB at Year 2

	Adj R^2	RMSE (cuft/acre)	Bias (cuft/acre)	MAPE (%)
Actual vs Projected Field Volume (Y=1344+0.78*X)	0.85	619.60	0.00	8.00
Actual vs Projected LiDAR Volume (Y=1125+0.73*X)	0.87	582.03	0.00	7.49

In the first regression model, which compares the Actual vs Projected plot Volume, the adj R^2 value is 0.85. This indicates that 85% of the variability in the actual TVOB can be explained by the Field projected TVOB. The root mean squared error (RMSE) of 619.60 cuft/acres provides a measure of the model's accuracy, with lower values indicating better performance. The bias is remarkably close to zero at 2.849498e-13, suggesting that, on average, the model predictions closely match the actual values. The mean absolute percentage error (MAPE) of 8% signifies that the model predictions, on average, deviate by 8% from the actual TVOB values.

In the second regression model, comparing the Actual vs Projected LiDAR Volume, the adj R^2 value is higher at 0.87. This model explains 87% of the variability in actual TVOB, indicating a stronger fit. The RMSE is 582.03 cuft/acres, which is slightly lower than the previous model, signifying improved accuracy. The bias is very close to zero as well, at 2.182343e-13, suggesting minimal prediction errors. The MAPE for this model is even lower, at 7.49%, indicating a slightly better average prediction accuracy than the first model.

Overall, these regression models show a good level of predictability for actual TVOB. The second model, involving LiDAR data, appears to outperform the first model in terms of explanatory power and prediction accuracy, as evidenced by the higher adj R^2 and lower RMSE and MAPE values.

Figures 2.3 and 2.4 depict the results of a regression analysis conducted between the observed TVOB and the predicted TVOB, utilizing estimated HD heights. In the actual vs. predicted plot, it becomes evident that the model tends to overestimate when the TVOB values are on the lower end and, conversely, underestimates when dealing with higher TVOB values. Figure 2.4 displays the residual plot of the regression, and it exhibits an absence of any discernible systematic pattern. This observation is indicative of the model holding to the assumption of normality. The lack of distinct trends or deviations in the residual plot suggests that the errors are randomly distributed and, therefore, the model predictions align with the normality assumption.

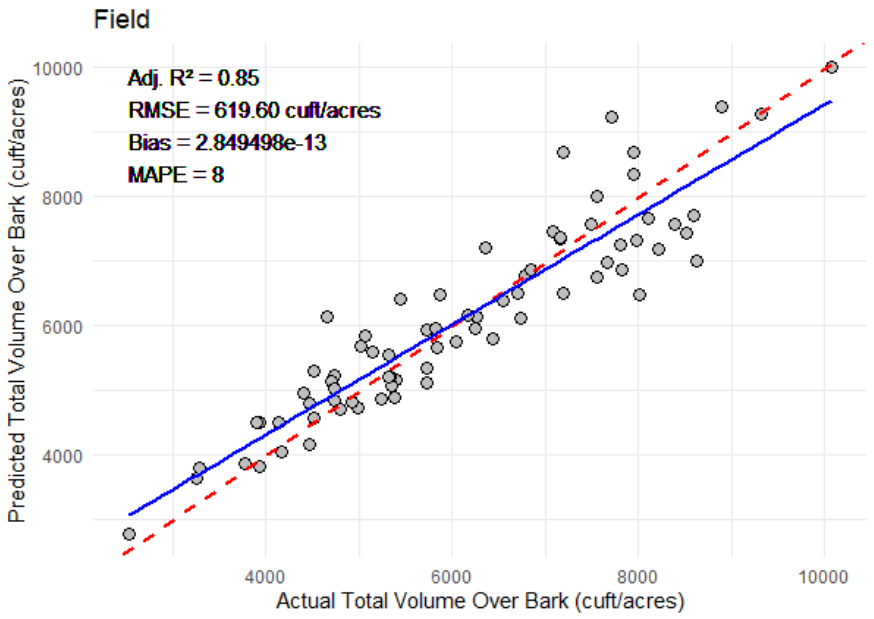

Figure 2. 3 Actual total volume over bark versus predicted total volume over bark by using field projected heights. The red dashed line shows a 1:1 line, while the blue solid line represents the regression line.

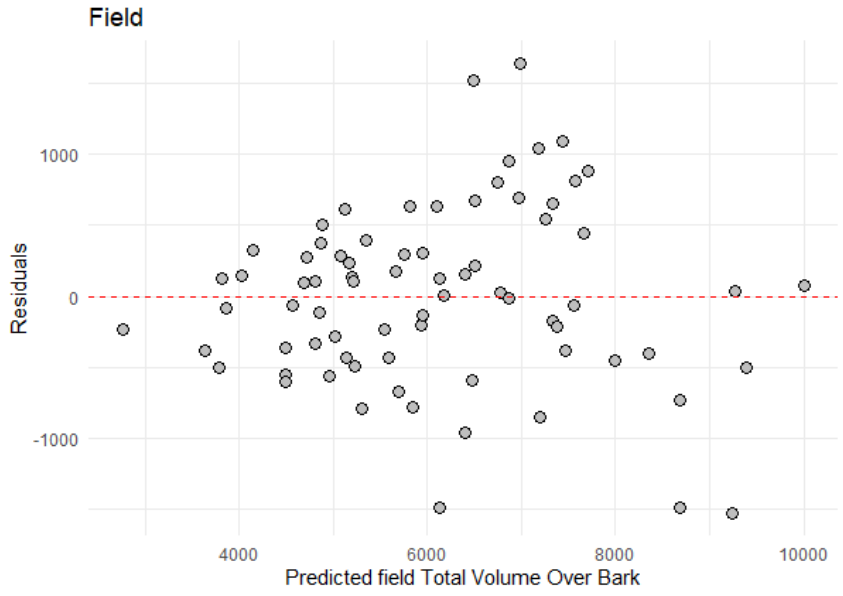

Figure 2. 4 Residual plot for predicted total volume over bark using projected field heights

Figures 2.5 and 2.6 present the outcomes of a regression analysis conducted to examine the relationship between actual TVOB and predicted TVOB values, using estimated LiDAR hmax heights as a predictor. In the actual vs. predicted plot, a noticeable trend emerges where the model consistently exhibits a tendency to overestimate TVOB when the actual values are at the lower end of the spectrum. Conversely, the model underestimates TVOB for cases involving higher TVOB values. Figure 27 showcases the residual plot resulting from the regression analysis. As the plot free of any visible systematic pattern, it suggests that the model conforms to the assumption of normality. The absence of distinct trends or deviations in the residual plot signifies that the model prediction errors are randomly distributed, aligning well with the normality assumption.

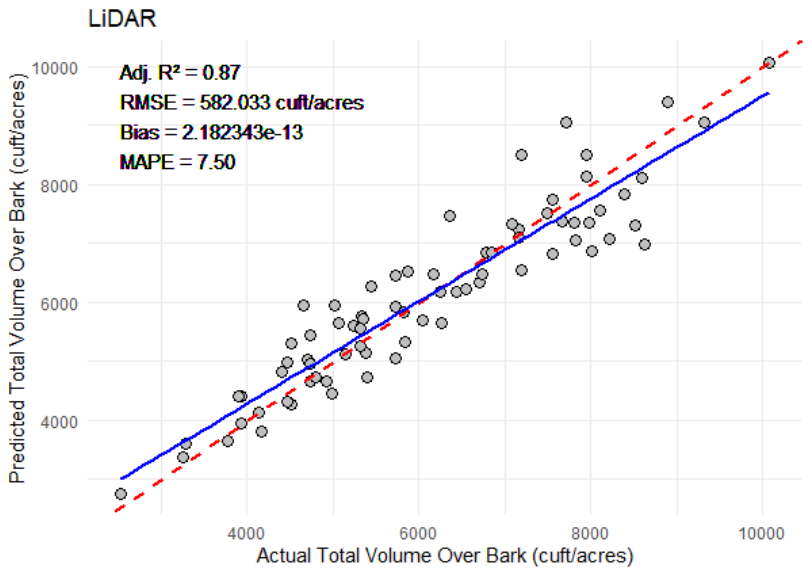

Figure 2. 5 Actual total volume over bark versus predicted total volume over bark by using LiDAR projected heights. The red dashed line shows a 1:1 line, while the blue solid line represents the regression line.

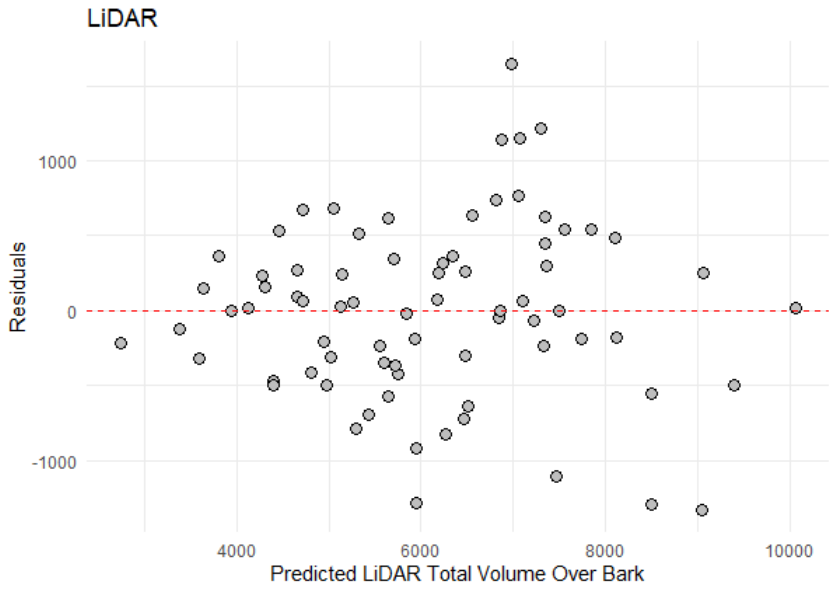

Figure 2. 6 Residual plot for predicted total volume over bark using projected LiDAR heights.

Model comparison for tree green weight:

Table 2.5 summarizes the linear regression analyses result, which investigate the relationship between actual Green Weight and two projection models: Actual vs Projected Field Green Weight and Actual vs Projected LiDAR Green Weight. These analyses assessed the models accuracy in predicting Green Weight, with a focus on the goodness of fit, prediction errors, an overall predictive performance.

Table 2. 5 Summary of Linear regression between Field projected GWOB and LiDAR projected GWOB with Actual GWOB at Year 2

	Adj R^2	RMSE (tons/acre)	Bias	MAPE (%)
Actual vs Projected Field Green Weight (Y=1344+0.78*X)	0.84	19.52	6.08E-13	8.43
Actual vs Projected LiDAR Green Weight (Y=1125+0.73*X)	0.85	18.63	-2.97E-14	8.18

In the first regression model, Actual vs Projected Field Green Weight, the Adj. R^2 is 0.84. This indicates that approximately 84% of the variance in actual Green Weight is explained by the model's predictions. The root mean squared error (RMSE), measuring the average prediction error, is 19.52 tons per acre. A lower RMSE suggests that the model is more accurate in its predictions. The bias is exceptionally close to zero, at -2.974673e-14, emphasizing the model capability to make predictions which closely align with actual values. The mean absolute percentage error (MAPE) of 8.43% means that, on average, the model predictions differ by 8.43% from the actual Green Weight values.

In the second regression model, Actual vs Projected LiDAR Green Weight, the Adj. R^2 value is slightly higher than the previous which is 0.85. The RMSE of 18.63 tons per acre is

marginally lower, indicating improved accuracy and a tighter fit between predicted and actual values for LiDAR projection heights. Remarkably, the bias is very close to zero, at -2.974673e-14, highlighting the model precision in predicting Green Weight. The MAPE is 8.18%, implying a slightly better average prediction accuracy compared to the first model. In summary, both models performed well in predicting Green Weight, with the second model exhibiting a slightly better goodness of fit and prediction accuracy.

Figures 2.7 and 2.8 summarize the results of a regression analysis between observed GWOB and predicted GWOB values using field HD heights as a predictor. In the actual vs. predicted plot, we see that the model consistently overestimates GWOB for lower values and underestimates it for higher values. Figure 2.8 shows the residual plot from the same analysis, and it doesn't show any kind of pattern which suggests that the model follows the assumption of normality.

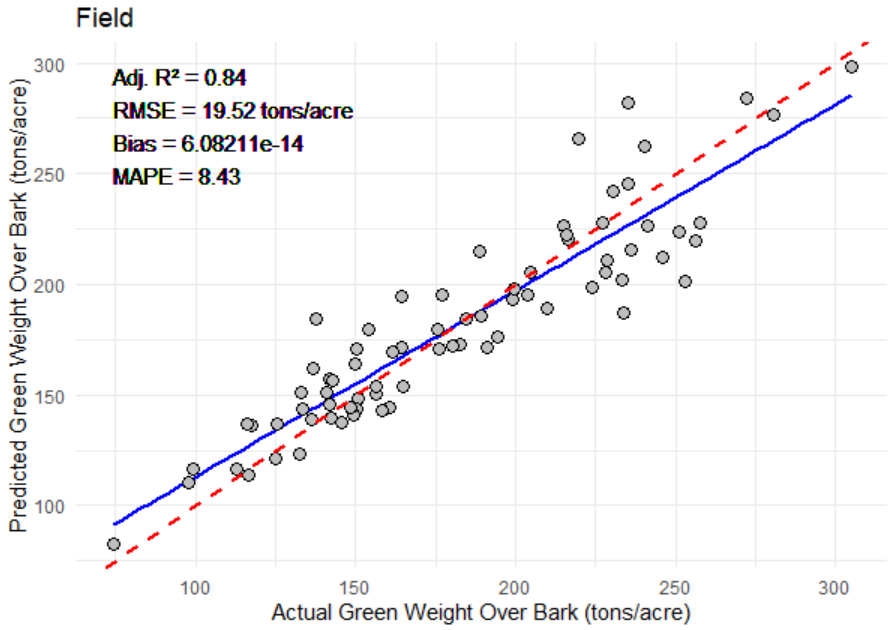

Figure 2. 7 Actual total volume over bark versus predicted total green weight over bark in tons/acre by using field projected heights. The red dashed line shows a 1:1 line, while the blue solid line represents the regression line.

Figure 2. 8 Residual plot for predicted total weight in tons/acre over bark using projected field heights

Similar to the field projected weight, Figures 2.9 and 2.10 describe a regression analysis comparing observed GWOB with predicted GWOB values using projected LiDAR HD heights. The model consistently overestimates GWOB for lower values and underestimates for higher values. In the residual plot (Figure 2.10), there is no obvious pattern, indicating that prediction errors are randomly distributed.

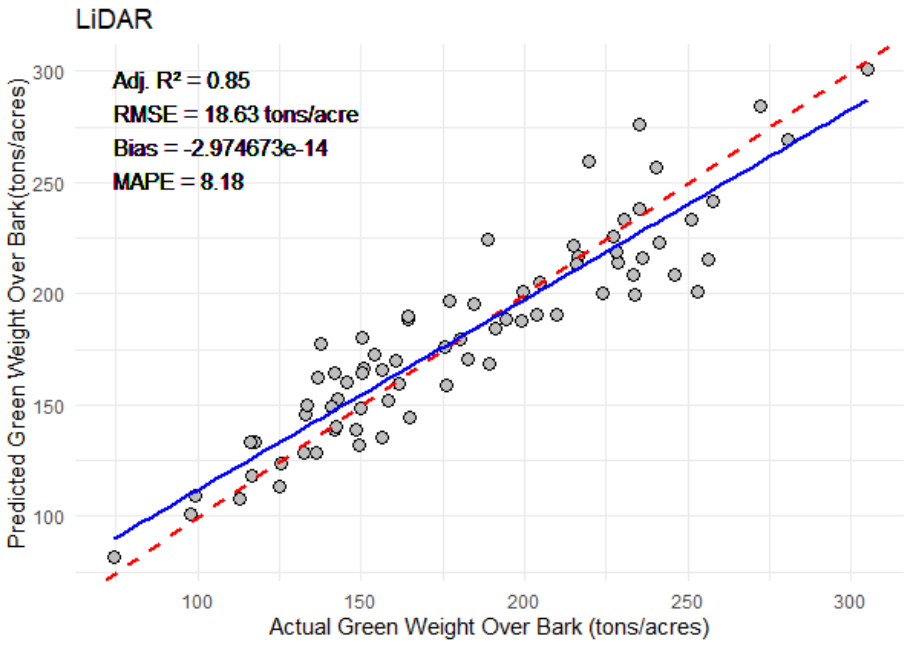

Figure 2. 9 Actual total volume over bark versus predicted total green weight over bark in tons/acre by using LiDAR projected heights. The red dashed line shows a 1:1 line, while the blue solid line represents the regression line.

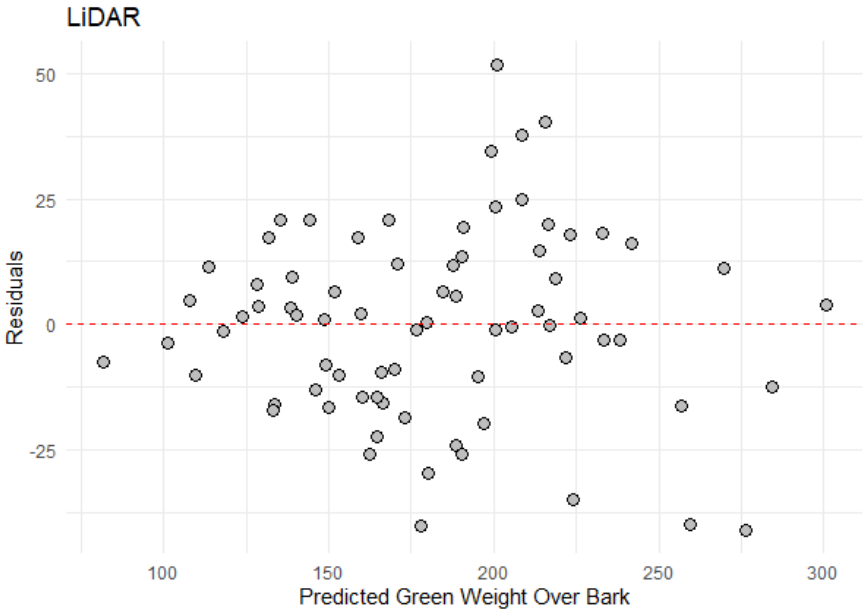

Figure 2. 10 Residual plot for predicted total weight in tons/acre over bark using projected LiDAR height.

5. DISCUSSION AND CONCLUSION:

This study presents a critical examination of LiDAR-derived projected heights as an efficient and innovative variable in the loblolly pine yield projection model. The utilization of LiDAR technology for projecting canopy heights opens new avenues in forest management and yields valuable insights into the optimization of prediction models. Traditionally, forest yield projection models have often relied on dominant height as an important parameter. However, the use of dominant height introduces challenges stemming from both subjectivity and inherent limitations. Dominant height calculations have historically been prone to human bias, introducing an element of variability that can compromise the accuracy of predictions (Yang & Burkhart, 2020). Furthermore, the conventional method of calculating dominant height, as exemplified in the PMRC height projection equation, averages tree heights that are greater than the mean diameter which neglects the plot-level variability. This optimal LiDAR Hmax key advantage is its consistency and its ability to capture data at a level of detail that is both systematic and unbiased, free from the influence of human judgment. This technological approach not only holds the promise of increased objectivity but also preserves the rich variability of tree heights throughout the entire plot, thus offering a comprehensive and more accurate representation of the forest ecosystem.

The study results have shown that while there is an insignificant difference between projected LiDAR tree heights from year 1 to year 2 and actual dominant height at year 2, there are instances of underestimation in LiDAR mean height. It is important to acknowledge that this discrepancy could be attributed to the use of a very low point density in LiDAR data, a factor noted in previous studies as well (Liu et al., 2007; C. A. Silva et al., 2017). These studies have highlighted

how lower point density LiDAR can result in underestimations of tree heights, and this consideration should guide future data collection practices.

To develop a robust and unbiased yield projection model for loblolly pine plantations, our study involved a comparative analysis of yield prediction models that employed field-projected heights and LiDAR-projected heights in relation to the actual yield data for the corresponding year. It is important to highlight that the actual yield data itself entailed a height simulation process, as destructive sampling was not performed. Despite this limitation, our findings demonstrated that the model utilizing LiDAR-projected Hmax heights outperformed the model based on field-projected data, exhibiting reduced errors in both TVOB and GWOB predictions. However, a noteworthy trend emerged within our results. As the volume and green weight increased, the model consistently tended to underestimate rather than overestimate. Intriguingly, this pattern was also evident in the field-based method, suggesting the possibility of irregularities in the actual data we used for comparison. It's essential to acknowledge that due to the absence of destructive sampling, this comparison method was our only option.

Yield prediction using LiDAR-based inventory attributes has a longstanding history in forest management. However, the recent development of lightweight and less complex UAVs equipped with laser technology has generated significant excitement within the field. Forest managers are keen to explore the operational potential of UAV LiDAR for more accurate and detailed assessments. One notable advantage of utilizing UAVs in LiDAR-based forest inventory is their ability to provide an exceptionally detailed scan of the forest (Wallace et al., 2012). This is largely attributed to their high point density resolution, which significantly enhances the efficiency and precision of predictive models. In contrast, Airborne Laser Scanning (ALS), while widely used, often falls short in terms of point density, consequently restricting the accuracy of

predictive models, as pointed out by Torresan et al. (2017). From our study, results showed that UAV LiDAR can be of more real estimation of 3D forest attributes and eventually for the prediction of volume and green weight. In our study, we have observed that UAV LiDAR can provide more accurate estimations of three-dimensional forest attributes. This enhanced precision carries significant implications for the reliable prediction of variables such as volume and green weight. The potential of UAV LiDAR to offer more realistic and detailed insights into forest parameters underscores its promise as a valuable tool for operational forest management and planning.

From these findings, a significant takeaway is that even with relatively low LiDAR point densities, it is feasible to construct effective yield projection models. The implications extend further: by acquiring higher LiDAR point densities, the potential for developing more detailed tree-level projection models becomes apparent. Prior research has already established the efficacy of increased point density for LiDAR applications, particularly in enhancing individual tree segmentation (Burt et al., 2018; Maggi et al., 2013).

Furthermore, the absence of GPS data for the dominant trees that were field measured limits the precision of our comparisons. The addition of GPS coordinates for these dominant trees would have enabled a more accurate assessment. This emphasizes the importance of early GPS data collection for individual trees inside inventory plots in plantation forests, as it can significantly enhance the accuracy and comprehensiveness of growth and yield estimates obtained through LiDAR remote sensing.

6. REFERENCES

- Ashton, P. S., & Liu, J. (1995). Individual-based simulation models for forest succession and management. *Forest Ecology & Management*, *73*(1-3), 157. https://doi.org/10.1016/0378-1127(94)03490-N
- Avery, T. E., & Burkhart, H. E. (1983). *Forest measurements* (3rd ed.) [Bibliographies
- Non-fiction]. McGraw-Hill. https://search.ebscohost.com/login.aspx?direct=true&AuthType=ip,shib&db=cat06564a&AN=uga.997790773902959&site=eds-live&custid=uga1
- Avery, T. E., & Burkhart, H. E. (2015). *Forest Measurements*. Waveland Press, Incorporated. https://books.google.com/books?id=_T1ArgEACAAJ
- Bettinger, P., Boston, K., Siry, J. P., & Grebner, D. L. (2016). *Forest management and planning*. Academic press.
- Bortolot, Z. J., & Wynne, R. H. (2005). Estimating forest biomass using small footprint LiDAR data: An individual tree-based approach that incorporates training data. *ISPRS Journal of Photogrammetry and Remote Sensing*, *59*(6), 342-360. https://doi.org/10.1016/j.isprsjprs.2005.07.001
- Brandtberg, T. (2003). Detection and analysis of individual leaf-off tree crowns in small footprint, high sampling density lidar data from the eastern deciduous forest in North America. *Remote Sensing of Environment*, *85*(3), 290-303. https://doi.org/10.1016/s0034-4257(03)00008-7
- Buchman, R. G., & Shifley, S. R. (1983). Guide to Evaluating Forest Growth Projection Systems. *Journal of Forestry*, *81*(4), 232-254. https://doi.org/10.1093/jof/81.4.232
- Burkhart, H., & Tomé, M. (2012). *Modeling Forest Trees and Stands*. https://doi.org/10.1007/978-90-481-3170-9
- Burt, A., Disney, M., Calders, K., & Goslee, S. (2018). Extracting individual trees from lidar point clouds using
- treeseg. *Methods in Ecology and Evolution*. https://doi.org/10.1111/2041-210x.13121
- Cao, L., Coops, N. C., Innes, J. L., Sheppard, S. R. J., Fu, L., Ruan, H., & She, G. (2016). Estimation of forest biomass dynamics in subtropical forests using multi-temporal airborne LiDAR data. *Remote Sensing of Environment*, *178*, 158-171. https://doi.org/10.1016/j.rse.2016.03.012
- Chapman, H. H., & Meyer, W. H. (1949). *Forest Mensuration*. McGraw-Hill. https://books.google.com/books?id=1uosAQAAMAAJ
- Chave, J., Rejou-Mechain, M., Burquez, A., Chidumayo, E., Colgan, M. S., Delitti, W. B., Duque, A., Eid, T., Fearnside, P. M., Goodman, R. C., Henry, M., Martinez-Yrizar, A., Mugasha, W. A., Muller-Landau, H. C., Mencuccini, M., Nelson, B. W., Ngomanda, A., Nogueira, E. M., Ortiz-Malavassi, E., . . . Vieilledent, G. (2014). Improved allometric models to estimate the aboveground biomass of tropical trees. *Glob Chang Biol*, *20*(10), 3177-3190. https://doi.org/10.1111/gcb.12629
- Chu, H.-J., Wang, C.-K., Huang, M.-L., Lee, C.-C., Liu, C.-Y., & Lin, C.-C. (2014). Effect of point density and interpolation of LiDAR-derived high-resolution DEMs on landscape

scarp identification. *GIScience & Remote Sensing*, *51*(6), 731-747. https://doi.org/10.1080/15481603.2014.980086

- Clutter, J. L., & Jones, E. P. (1980). *Prediction of growth after thinning in old-field slash pine plantations* (Vol. 217). Department of Agriculture, Forest Service, Southeastern Forest Experiment ….
- De Frenne, P., Zellweger, F., Rodríguez-Sánchez, F., Scheffers, B. R., Hylander, K., Luoto, M., Vellend, M., Verheyen, K., & Lenoir, J. (2019). Global buffering of temperatures under forest canopies. *Nature Ecology & Evolution*, *3*(5), 744-749.
- Eugene, A. T., & E., B. H. (1983). Forest measurements. 3rd ed.
- Harrison, W. M., & Borders, B. E. (1996). Yield prediction and growth projection for site-prepared loblolly pine plantations in the Carolinas, Georgia, Alabama, and Florida. https://doi.org/http://pmrc.uga.edu/TR1996-1.pdf
- Haynes, R. W. (2003). *An analysis of the timber situation in the United States: 1952 to 2050* (Vol. 560). US Department of Agriculture, Forest Service, Pacific Northwest Research Station.
- Heurich, M., Persson, Å., Holmgren, J., & Kennel, E. (2004). Detecting and measuring individual trees with laser scanning in mixed mountain forest of central Europe using an algorithm developed for Swedish boreal forest conditions. *International Archives of Photogrammetry, Remote Sensing and Spatial Information Sciences*, *36*(Part 8), W2.
- Hopkinson, C., Chasmer, L., & Hall, R. J. (2008). The uncertainty in conifer plantation growth prediction from multi-temporal lidar datasets. *Remote Sensing of Environment*, *112*(3), 1168-1180. https://doi.org/10.1016/j.rse.2007.07.020
- Hudak, A. T., Evans, J. S., & Stuart Smith, A. M. (2009). LiDAR utility for natural resource managers. *Remote Sensing*, *1*(4), 934-951.
- Jeffrey P. Prestemon, R. C. A. (2002). *Timber products supply and demand. In: Wear, D.N.; Greis, J.G., eds.*
- JMP®17. (2022). *JMP Statistical Discovery LLC 2022*. In
- Kwak, D.-A., Lee, W.-K., Lee, J.-H., Biging, G. S., & Gong, P. (2007). Detection of individual trees and estimation of tree height using LiDAR data. *Journal of Forest Research*, *12*(6), 425-434. https://doi.org/10.1007/s10310-007-0041-9
- LidarExplorer, U. https://apps.nationalmap.gov/lidar-explorer/#/
- Maggi, K., Qinghua, G., Wenkai, L., & Marek, K. J. (2013). Delineating Individual Trees from Lidar Data: A Comparison of Vector- and Raster-based Segmentation Approaches [article]. *Remote Sensing*, *5*(9), 4163-4186. https://doi.org/10.3390/rs5094163
- Maltamo, M., Eerikäinen, K., Pitkänen, J., Hyyppä, J., & Vehmas, M. (2004). Estimation of timber volume and stem density based on scanning laser altimetry and expected tree size distribution functions [Article]. *Remote Sensing of Environment*, *90*(3), 319-330. https://doi.org/10.1016/j.rse.2004.01.006
- Matti Maltamo, E. N., Jari Vauhkonen. (2014). *Forestry applications of airborne laser scanning: Concepts and case studies*. Springer Dordrecht. https://doi.org/https://doi.org/10.1007/978-94-017-8663-8
- Munro, D. D. (1974). Forest growth models-a prognosis. In *Growth models for tree and stand simulation* (Vol. 30, pp. 7-21). Research Note 30. Department of Forest Yield Research, Royal College of ….

- Naesset, E. (1997). Determination of mean tree height of forest stands using airborne laser scanner data. *52*(2), 49-56. https://search.ebscohost.com/login.aspx?direct=true&AuthType=ip,shib&db=edsbl&AN=RN024544941&site=eds-live&custid=uga1
- Nelson, R. (1997). Modeling forest canopy heights: The effects of canopy shape. *Remote Sensing of Environment*, *60*(3), 327-334.
- Nelson, R., Jimenez, J., Schnell, C. E., Hartshorn, G. S., Gregoire, T. G., & Oderwald, R. (2010). Technical note: Canopy height models and airborne lasers to estimate forest biomass: Two problems. *International Journal of Remote Sensing*, *21*(11), 2153-2162. https://doi.org/10.1080/01431160050029486
- Nepal, S. K., & Somers, G. L. (1992). A generalized approach to stand table projection. *Forest science*, *38*(1), 120-133.
- Pienaar, L. V., Burgan, T., & Rheney, J. W. (1987). *Stem volume, taper and weight equations for site-prepared loblolly pine plantations*. Plantation Management Research Cooperative, School of Forest Resources ….
- Pienaar, L. V., & Harrison, W. M. (1989). A STAND TABLE PROJECTION APPROACH TO YIELD PREDICTION IN UNTHINNED, EVEN-AGED STANDS[1]. Proceedings of the Fifth Biennial Southern Silvicultural Research Conference: Memphis, Tennessee, November 1-3, 1988,
- Plowright, A., & Roussel, J. (2018). ForestTools: analyzing remotely sensed forest data. *R Package Version 0.2. 0*.
- Popescu, S. C. (2007). Estimating biomass of individual pine trees using airborne lidar. *Biomass and Bioenergy*, *31*(9), 646-655. https://doi.org/10.1016/j.biombioe.2007.06.022
- Popescu, S. C., Wynne, R. H., & Nelson, R. F. (2002). Estimating plot-level tree heights with lidar: local filtering with a canopy-height based variable window size. *Computers and electronics in agriculture*, *37*(1-3), 71-95.
- Popescu, S. C., & Zhao, K. (2008). A voxel-based lidar method for estimating crown base height for deciduous and pine trees. *Remote Sensing of Environment*, *112*(3), 767-781. https://doi.org/10.1016/j.rse.2007.06.011
- Pretzsch, H. (2010). *Forest Dynamics, growth and yield from measurement to model*. Springer. https://doi.org/https://doi.org/10.1007/978-3-540-88307-4
- Puettmann, K. J., Wilson, S. M., Baker, S. C., Donoso, P. J., Drössler, L., Amente, G., Harvey, B. D., Knoke, T., Lu, Y., & Nocentini, S. (2015). Silvicultural alternatives to conventional even-aged forest management-what limits global adoption? *Forest Ecosystems*, *2*(1), 1-16.
- R Core Team, R. (2022). R: A language and environment for statistical computing. https://www.R-project.org/
- Robinson, A. P., & Monserud, R. A. (2003). Criteria for comparing the adaptability of forest growth models [Article]. *Forest Ecology and Management*, *172*(1), 53-67. https://doi.org/10.1016/S0378-1127(02)00041-5
- Roise, J. P., Harnish, K., Mohan, M., Scolforo, H., Chung, J., Kanieski, B., Catts, G. P., McCarter, J. B., Posse, J., & Shen, T. (2016). Valuation and production possibilities on a working forest using multi-objective programming, Woodstock, timber NPV, and carbon storage and sequestration. *Scandinavian Journal of Forest Research*, *31*(7), 674-680. https://doi.org/10.1080/02827581.2016.1220617

- Roussel, J.-R., Auty, D., Coops, N. C., Tompalski, P., Goodbody, T. R., Meador, A. S., Bourdon, J.-F., De Boissieu, F., & Achim, A. (2020). lidR: An R package for analysis of Airborne Laser Scanning (ALS) data. *Remote Sensing of Environment*, *251*, 112061.
- Samuelson, P. A. (1976). Economics of Forestry in an Evolving Society. *Economic Inquiry*, *14*(4), 466-492. https://doi.org/10.1111/j.1465-7295.1976.tb00437.x
- Sarkar, D. (2008). Lattice: Multivariate Data Visualization with {R}. *Springer*. http://lmdvr.r-forge.r-project.org
- Schumacher, F. X., & Hall, F. d. S. (1933). Logarithmic expression of timber-tree volume.
- Silva, C., Klauberg, C., Hudak, A., Vierling, L., Jaafar, W., Mohan, M., Garcia, M., Ferraz, A., Cardil, A., & Saatchi, S. (2017). Predicting Stem Total and Assortment Volumes in an Industrial Pinus taeda L. Forest Plantation Using Airborne Laser Scanning Data and Random Forest. *Forests*, *8*(7). https://doi.org/10.3390/f8070254
- Silva, C. A., Klauberg, C., Hudak, A. T., Vierling, L. A., Jaafar, W. S. W. M., Mohan, M., Garcia, M., Ferraz, A., Cardil, A., & Saatchi, S. (2017). Predicting stem total and assortment volumes in an industrial Pinus taeda L. forest plantation using airborne laser scanning data and random forest [Journal Article]. *Forests*, *8*(7), 254. https://doi.org/10.3390/f8070254
- https://www.mdpi.com/1999-4907/8/7/254/htm
- Tesfamichael, S. G., Ahmed, F. B., & Van Aardt, J. A. N. (2010). Investigating the impact of discrete-return lidar point density on estimations of mean and dominant plot-level tree height in Eucalyptus grandis plantations. *International Journal of Remote Sensing*, *31*(11), 2925-2940. https://doi.org/10.1080/01431160903144086
- Thomas, V., Treitz, P., McCaughey, J. H., & Morrison, I. (2006). Mapping stand-level forest biophysical variables for a mixedwood boreal forest using lidar: an examination of scanning density. *Canadian Journal of Forest Research*, *36*(1), 34-47.
- Weiskittel, A. R. (2011). *Forest growth and yield modeling* [Bibliographies
- Non-fiction]. Wiley. https://search.ebscohost.com/login.aspx?direct=true&AuthType=ip,shib&db=cat06564a&AN=uga.9939510163902959&site=eds-live&custid=uga1
- Wickham, H. (2011). ggplot2. *Wiley interdisciplinary reviews: computational statistics*, *3*(2), 180-185.
- Wulder, M. A., White, J. C., Nelson, R. F., Næsset, E., Ørka, H. O., Coops, N. C., Hilker, T., Bater, C. W., & Gobakken, T. (2012). Lidar sampling for large-area forest characterization: A review. *Remote Sensing of Environment*, *121*, 196-209. https://doi.org/https://doi.org/10.1016/j.rse.2012.02.001
- Yang, S.-I., & Burkhart, H. E. (2020). Evaluation of total tree height subsampling strategies for estimating volume in loblolly pine plantations. *Forest Ecology and Management*, *461*. https://doi.org/10.1016/j.foreco.2020.117878
- Zhang, W., Qi, J., Wan, P., Wang, H., Xie, D., Wang, X., & Yan, G. (2016). An Easy-to-Use Airborne LiDAR Data Filtering Method Based on Cloth Simulation. *Remote Sensing*, *8*(6). https://doi.org/10.3390/rs8060501

CHAPTER 3

MODELING STAND VOLUME AND GREEN WEIGHT BY UTILIZING HIGH-RESOLUTION UAV-DERIVED LIDAR DATA IN LOBLOLLY PINE PLANTATIONS

1. BACKGROUND:

Loblolly pine is one of the most important commercial pines for the plantation industry in the southeast USA and planted more than other species (Thompson, 1998). Their extent has been increasing and volume of harvested product of this species is also increasing through time with declining age for thinning commercially. There are many theories for explaining this which say that southern pine grows at a greater rate than other pines in the world. For example, many others have reported that controlling competing vegetation is resulting in increase of this growth rate (Miller et al., 1991; Pienaar & Shiver, 1993), or genetic improvement in the seed as seedling quality improves growth rate too (Buford & Burkhart, 1987; McKeand, 2019). Fertilization also has played promising role in diameter growth and volume growth of loblolly plantation (Sayer et al., 2004).

As southern pine has proven to be a commercially important plant, an accurate growth and yield prediction system to predict the expected outcomes, forecast policies and alternatives for its growth is a must. This is very critical for forest managers. Growth and yield of volume or green weight are generally functions of site quality, stand age, and stand density. Traditional inventory

is generally done to get required attributes to get the information required to formulate these attributes.

Common measurement taken from inventory are diameter at breast height (DBH), tree density, site quality, and stem quality (Avery & Burkhart, 2015). But when it comes to measuring tree heights, it's already established that the traditional method of getting it is very imprecise and biased. Eventually it has led to unreliable and unrealistic tree volume with associated error. Apart from that, measuring tree attributes again and again can be very costly and there are many problems of having lack of trained people to do that. To reduce cost, time and be efficient, forest managers started using subsampling of dominant and codominant tree heights and eventually used a height and diameter relationship to estimate the height of remaining trees of plot (Arabatzis & Burkhart, 1992). When fitting models for volume or weight, the independent variables are considered free from measurement error. However, it is not possible in the traditional based inventory estimates.

Light Detection and Ranging (LiDAR) can provide a solution to this problem. There has been studies done in very early days where researchers have used laser data to estimate forest attributes (Nelson, Krabill, & MacLean, 1984; Nelson, Oderwald, & Gregoire, 1997). LiDAR systems are generally of two types (1) aerial and (2) terrestrial. Both types were successfully used to estimate volume and biomass in pine plantations (Edson & Wing, 2011; Maltamo et al., 2004; Zhao et al., 2018; Zolkos, Goetz, & Dubayah, 2013), using lidar derived heights, intensity, and canopy cover metrics (Næsset, 1997b; Ross Nelson, 1988). While height is one of the most important variables, canopy profile also showed to be highly related with timber volume (Nilsson, 1996). In aerial laser, there are two types of scanners: (1) Airborne Laser Scanner (ALS) and (2) Unmanned Aerial Vehicle (UAV) lidar systems. ALS has been extensively used for different forest

inventories attributes (Hyyppä et al., 2017). However, with advancement of LiDAR, UAV has been offering increased accuracy because of its relatively low cost and high resolution as it flies near tree height (Rothmund, Vouillamoz, & Joswig, 2017). As UAV has an increased number of returns, the intensity and shape of a tree is also clear, potentially helping for individual tree level research as well. LiDAR technology has a long-standing history in applications related to loblolly pine, with various studies assessing it for attribute estimation. For instance, Duncanson et al. (2015); Srinivasan et al. (2014); Sumnall et al. (2021) have employed LiDAR to assess biomass and understory characteristics. Moreover, validating individual-level volume measurements through LiDAR against traditional cruise and felled tree methods has strongly indicated the effectiveness of LiDAR in characterizing forest volume within loblolly pine plantations, as highlighted by (Corrao, Sparks, & Smith, 2022). Sumnall et al. (2022) has utilized UAV to delineate individual tree and then estimate volume and diameter using near accurate estimates to field measurements.

However, the exploration of UAV LiDAR at the stand level for volume and growth estimates within loblolly pine plantations has remained relatively new. Therefore, this study employs a high point density UAV LiDAR system to provide more accurate estimates of volume and green weight for loblolly pine plantations. The primary objective of this research is to investigate how LiDAR-derived tree metrics can successfully contribute to the accuracy of laser data in relation to loblolly plantation yield estimates.

2. OBJECTIVES:

- To develop a UAV LiDAR-based model for estimating total volume over bark
- To create a UAV LiDAR-based model for estimating total green weight over bark

3. MATERIAL AND METHODS:

Study sites used for this chapter are the same as for chapters 1 and 2.

Field data:

In this study, we utilized the Total Volume Over Bark (TVOB) and Green Weight Over Bark (GWOB) values that were calculated using the PMRC 2016 model, as outlined in Borders et al. (2014). Access to this model is exclusively granted to members of the PMRC, and, in compliance with these restrictions, we relied solely on the provided values for our comparative analysis. The total numbers of plot and age range of this field data was same as the data from year 3 of field data in chapter 1. The plot size was in the range of 0.3-0.6 acres.

Table 3. 1 Summary statistics of TVOB and GWOB from field data

Statistic	*Total Volume Over Bark (cuft/acre)*	*Green Weight Over Bark (tons/acre)*
Mean	6,617.25	201.71
SD	2,312.04	74.36
Max	11,398.90	356.30
Min	2,365.70	69.40

The descriptive statistics summary of these values is presented in table 3.1 above. The mean TVOB, representing the average total volume of wood over bark in cubic ft per acre, is approximately 6,617.25 cuft/acre, while the mean GWOB, signifying the average green weight per plot over bark in tons per acre, is approximately 201.71 tons/acre. Additionally, the Standard Deviation (SD), which for TVOB is approximately 2,312.04 and for GWOB is about 74.36,

signifying the degree of variability or spread in the data. The Maximum (Max) values, 11,398.90 cuft/acre for TVOB and 356.30 tons/acre for GWOB, while the Minimum (Min) values, 2,365.70 cuft/acre for TVOB and 69.40 tons/acre for GWOB. These statistics collectively offer a comprehensive overview of the dataset's central tendencies, variability, and range in TVOB and GWOB values, forming a critical foundation for our comparative analysis.

LiDAR data:

The LiDAR data employed in this chapter builds upon the dataset introduced in Chapter 1, which was obtained with a lidar sensor onboard an Unmanned Aerial Vehicle (UAV). A comprehensive description of the UAV, sensor, and data extraction process can be found in the UAV section of the LiDAR data methods in Chapter 1. The dataset comprises 3D LiDAR points collected from various plots. To extract valuable insights from the LiDAR data, a set of standard LiDAR metrics per plot was computed in R using LidR library. These metrics serve as vital indicators of the tree's structural characteristics. The calculated LiDAR metrics encompass a wide range of attributes: The LiDAR metrics encompass several categories. The Echo Height Metrics provide insights into the vertical distribution of vegetation, including HMAX (Maximum Height), HMEAN (Mean Height), HMEDIAN (Median Height), HSD (Standard Deviation of Heights), HVAR (Variance of Heights), HCV (Coefficient of Variation of Heights), HKUR (Kurtosis of Heights), and HSKE (Skewness of Heights). Height percentiles reveal detailed height distributions, ranging from H01TH to H99TH. The Canopy Relief Ratio indicates canopy cover and structural complexity. Intensity metrics, including ISD (Standard Deviation of LiDAR Intensity), IVAR (Variance of LiDAR Intensity), ICV (Coefficient of Variation of LiDAR Intensity), IKUR (Kurtosis of LiDAR Intensity), and ISKE (Skewness of LiDAR Intensity), depict

LiDAR intensity distribution. Lastly, percentage metric depicts the distribution of first returns above specific height thresholds and considers all returns, including that above minimum, mean, and mode height values.

Table 3. 2 List of LiDAR metrics extracted and used for model evaluation

Abbreviation	Description (plot)
HMAX, HMEAN, HMEDIAN, HSD, HVAR, HCV, HKUR, HSKE	Echo Height Metrics
H01TH, H05TH, H10TH, H15TH……...H99TH	Height percentiles
Canopy.Relief.Ratio	(mean height - minimum height) / (maximum height - minimum height)
ISD, IVAR,ICV,IKUR,ISKE	Intensity Metrics
Percentage.first.returns.above.2, Percentage.first.returns.above.mean, Percentage.first.returns.above.mode,	Percentage of first return above minimum, mean and mode height values
Percentage.all.returns.above.2 Percentage.all.returns.above.mean Percentage.all.returns.above.mode	Proportion of all above minimum, mean and mode height values

Statistical Modeling:

To model volume and green weight per acre using LiDAR metrics, we have selected the LASSO (Least Absolute Shrinkage and Selection Operator) regression technique for several compelling reasons. Firstly, LASSO's unique ability to perform feature selection and regularization is important in the context of LiDAR metrics, which often include a multitude of variables. This vast array of metrics necessitates a careful selection of the most significant ones for our yield modeling. LASSO's effectiveness in automatically identifying and emphasizing a subset of the most relevant metrics stems from its incorporation of an L1 regularization term. This regularization not only penalizes large coefficients but also prevents the model from inadvertently

capturing extraneous noise and random variations within the metrics, rendering it more robust and dependable. Specifically, LASSO zeroes in on irrelevant metrics, thus simplifying the model and enhancing its reliability.

Moreover, LASSO exhibits proficiency in addressing the prevalent issue of multicollinearity, which frequently plagues LiDAR data, originating from the vertical scan of laser points. The conventional linear regression approach assumes that predictor variables should be free from multicollinearity, making it challenging for LiDAR data. LASSO adeptly overcomes this challenge by singling out a feature from a set of correlated ones and rendering the coefficients of the remaining features to zero, preserving the model stability and dependability. Notably, a study conducted by demonstrated the enhanced accuracy of the LASSO method when compared to other modeling techniques, including Least Squares Regression (LSR), Random Forest (RF), and Generalized Additive Modeling Selection (GAMSEL).

To optimize the LASSO model, we employed a k-fold cross-validation approach to determine the best λ, which signifies the shrinkage amount, particularly employing a 10-fold cross-validation scheme. In this method, our dataset was randomly partitioned into ten equally sized sub-samples, with nine being dedicated to model development and one for model validation. This process was iterated ten times, with each sub-sample taking a turn as the validation set. The final model was then developed by combining the results obtained from each iteration of the validation process. The "glmnet" package in R was utilized to perform this analysis, ensuring a robust and optimized LASSO model. The accuracy of the model was tested using metrics such as adjusted R^2, Root Mean Sum of Square (RMSE), Mean Bias Error (Bias) and Akaike Information Criterion (AIC).

4. RESULT:

In our initial LASSO model, over 15 variables were selected for both green weight and volume predictions. However, upon closer examination, we found that a significant portion of these variables were primarily derived from a single LiDAR return or were closely linked to specific sensor characteristics. Therefore, we opted to refine our model by removing variables such as HMAX, HMODE, HMEDIAN, and certain percentage values.

Instead, we focused on incorporating variables that represent a broader range of values and are considered standard parameters applicable to various field conditions. This approach ensures that our models can be more easily replicated by other studies, regardless of the specific sensors used or the field conditions in which the UAVs were deployed.

While this adjustment may have involved a slight compromise in terms of model accuracy, we recognized that a more parsimonious model, with a reduced number of parameters, often yields more robust and interpretable results. In this way, we aimed to strike a balance between model simplicity and predictive power.

Table 3. 3 Estimate summary of derived LiDAR attributes.

Metrics	Mean	SD	Max	Min
HMAX	93.43	7.21	104.4	68.93
HMEAN	73.71	9.04	88.58	48.06
HMODE	76.9	11.76	91.11	4.69
HMEDIAN	76.25	7.94	89.8	52.99
HSD	11.88	4.06	25.66	7.55
HVAR	47.98	36.63	200.49	17.32
HCV	55.41	26.49	175.07	27.92
HKUR	50	21.2	98.79	6.43

HSKE	-8.95	2.07	-2.72	-13.32
H01TH	25.62	17.73	60.17	4.63
H05TH	51.65	21.26	78.38	5.15
H10TH	60.72	17.41	81.63	5.91
H15TH	66.27	12.47	83.53	6.82
H20TH	68.8	11.2	84.91	8.23
H25TH	70.4	10.81	86.02	12.24
H30TH	72.16	8.55	86.94	46.72
H35TH	73.36	8.24	87.73	49.93
H40TH	74.4	8.11	88.45	51.02
H45TH	75.35	8	89.11	52.07
H50TH	76.25	7.94	89.8	52.99
H55TH	77.11	7.88	90.52	53.81
H60TH	77.96	7.82	91.21	54.66
H65TH	78.81	7.76	91.93	55.54
H70TH	79.68	7.71	92.62	56.4
H75TH	80.58	7.66	93.34	57.25
H80TH	82.62	7.57	94.82	59.35
H90TH	83.91	7.52	95.77	60.66
H95TH	85.71	7.46	97.11	62.37
H99TH	88.67	7.38	100.07	65.19
Canopy.relief.ratio	0.78	0.05	0.86	0.57
ISD	17.45	1.51	20.69	15.43
IVAR	306.62	54.87	428.04	238.22
ICV	45.71	2.92	51.61	40.92
IKUR	2.34	0.42	3.14	1.77
ISKE	0.05	0.28	0.51	-0.48
Pentage.first.returns.Above.2	76.34	14.42	92.95	33.23
Percentage.all.returns.above.2	76.35	14.42	92.97	33.24
Percentage.first.returns.above.mode	32.08	8.77	52.92	13.05
Percentage.all.returns.above.mean	46.55	9.54	65.52	19.42
Percentage.all.returns.above.mode	33.51	9.25	53.76	13.54

Model for total volume over bark (TVOB):

The Pearson correlation coefficient was run with the parameter selected from TVOB lasso regression model. The results are shown in figure 3.1 below:

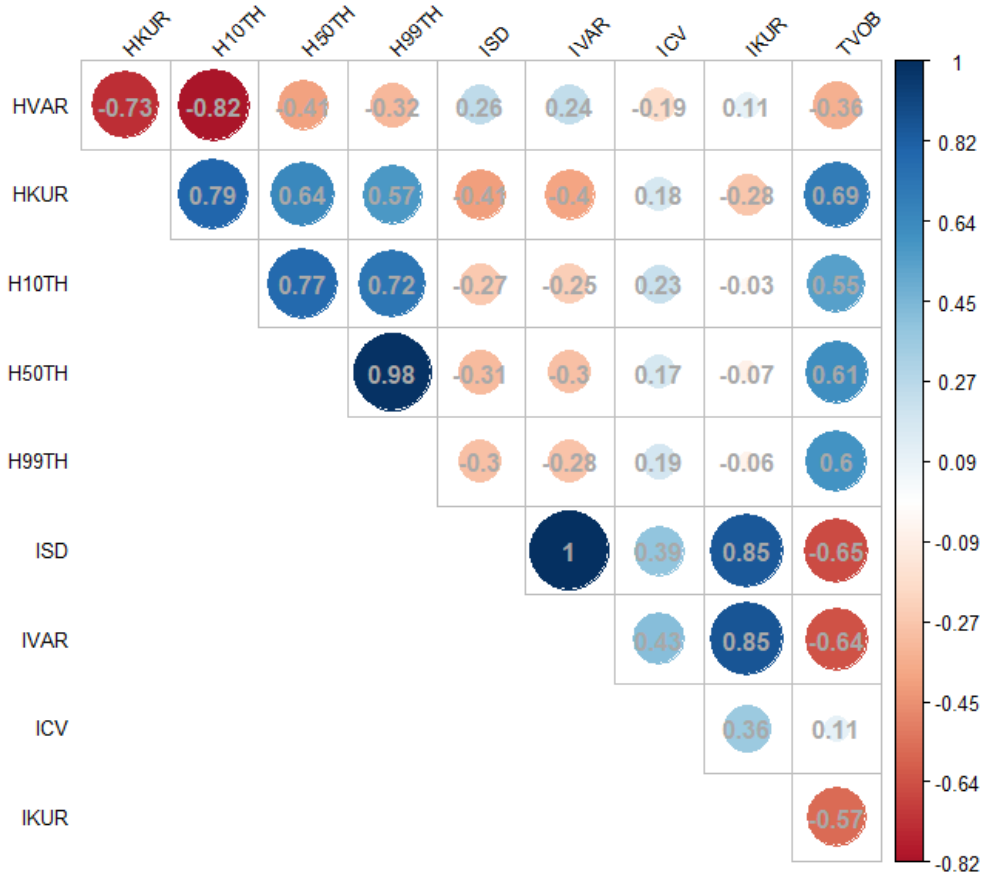

Figure 3. 1 Pearson correlation matrix of variables selected with dependent variable, total volume over bark estimated from the field meaasurements.

Table 3. 4 Variables selected in the TVOB regression model, along with their corresponding coefficients.

Variable	*Coefficient*
(Intercept)	6617.25
HVAR	884.12
HKUR	937.59
H10TH	701.78
H50TH	147.21
H99TH	115.34
ISD	-640.21
IVAR	-38.29
ICV	564.76
IKUR	-725.20

Table 3.4 provides an overview of the variable with coefficients derived from the Lasso regression model, which explores the relationships between the PMRC 2016 TVOB per acre and a range of UAV LiDAR metrics. Each coefficient corresponds to a specific UAV LiDAR metric and represents the estimated impact of that metric on the TVOB. Positive coefficients suggest a positive relationship, implying that an increase in the UAV LiDAR metric is associated with an increase in volume. Conversely, negative coefficients indicate a negative relationship, where an increase in the UAV LiDAR metric shows a decrease in TVOB. These coefficients play a pivotal role in understanding the quantitative influence of individual UAV LiDAR metrics on the PMRC 2016 volume, shedding light on the critical features contributing to the observed variability.

For instance, the HVAR coefficient of 884.12 indicates a positive influence of the height variance on TVOB (cubic ft per acre). In practical terms, this means that as the maximum height value from UAV LiDAR data increases, the volume tends to increase as well. Conversely, the

"ISD" coefficient of -640.21 signifies a negative relationship, suggesting that higher values of the intensity standard deviation metric are associated with lower volume. These coefficients offer precise insights into the strength and direction of these relationships, allowing for a more informed interpretation of the influence of UAV LiDAR metrics on the forest stand volume.

Table 3. 5 Adjusted R^2, RMSE (Root Mean Square Error), Mean Bias Error (Bias), and AIC (Akaike Information Criterion) values for both the LASSO TVOB best model and the cross-validation model

RMSE (cuft/acre)		**Adj. R2**		**Bias (cuft/acre)**		**AIC**
Best_model	CV	Best_model	CV	Best_model	CV	
1077.02	1177.06	0.78	0.75	-5.42E-13	-2.41E-13	-2.79E+08

The results for the best model for TVOB had adjusted R-squared (Adj. R^2) value of 0.78 (n=68) indicates that approximately 78% of the variance observed in the PMRC 2016 total volume per acre can be explained by the UAV LiDAR metrics. Similarly, the Root Mean Square Error (RMSE) of 1077.02 cuft/acre, in conjunction with the minimal mean bias error, underscores the model remarkable capacity to minimize bias in its predictions. In the cross-validation dataset, the model maintains a commendable performance with an R^2 value of 0.75 and an RMSE of 1177.06 cuft/acre, with negligible bias. The Akaike Information Criterion (AIC) provides further validation, indicating the model's aptness in explaining the data while preserving parsimony.

Visualizing the observed versus predicted TVOB through the figure (3.1) underscores the model effectiveness. The residual plot and histogram displayed in the figure offer additional insights. They explain the absence of any patterns and highlight the model efficacy in capturing the variance inherent in the utilized data, further confirming the model robust performance and reliability.

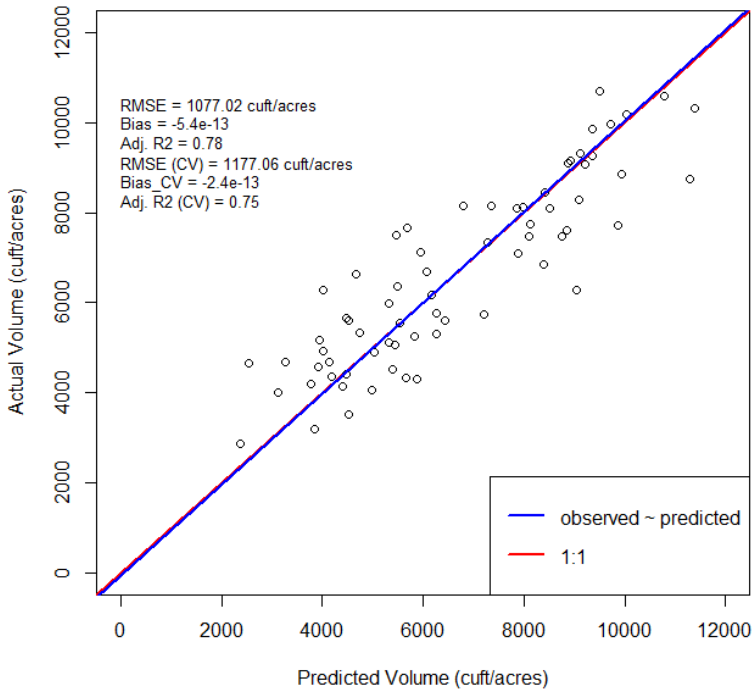

Figure 3. 2 Scatter plot depicting the comparison between predicted and actual volume (cu ft per acre) obtained from the best model. The red line is 1:1, blue line represents the regression line between actual volume and predicted volume from the model.

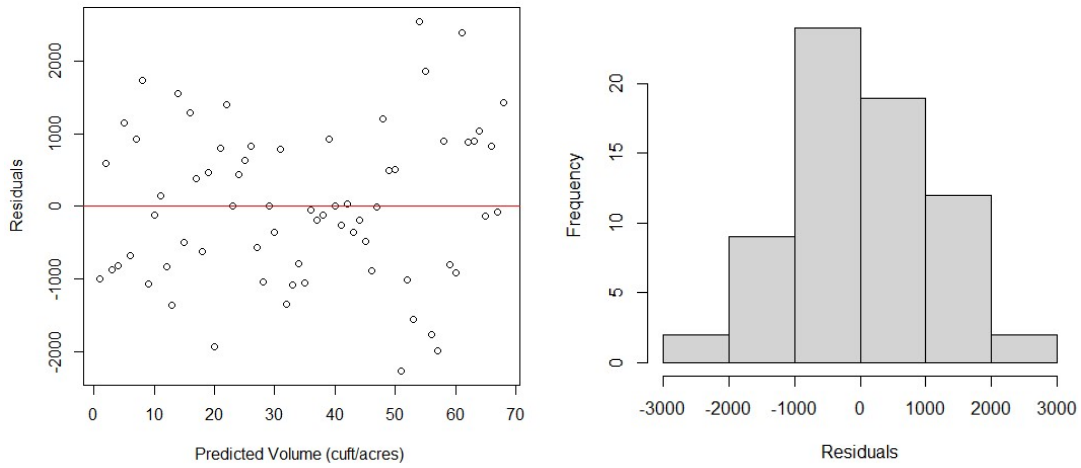

Figure 3. 3 Residual versus predicted values for the TVOB model on the left side, and a histogram illustrating the distribution of residuals on the right side

Model for Green Weight Over Bark (GVOB):

The Pearson correlation coefficient was calculated using the parameter chosen from the green weight LASSO regression model, and the outcomes are displayed in the figure (3.4) below:

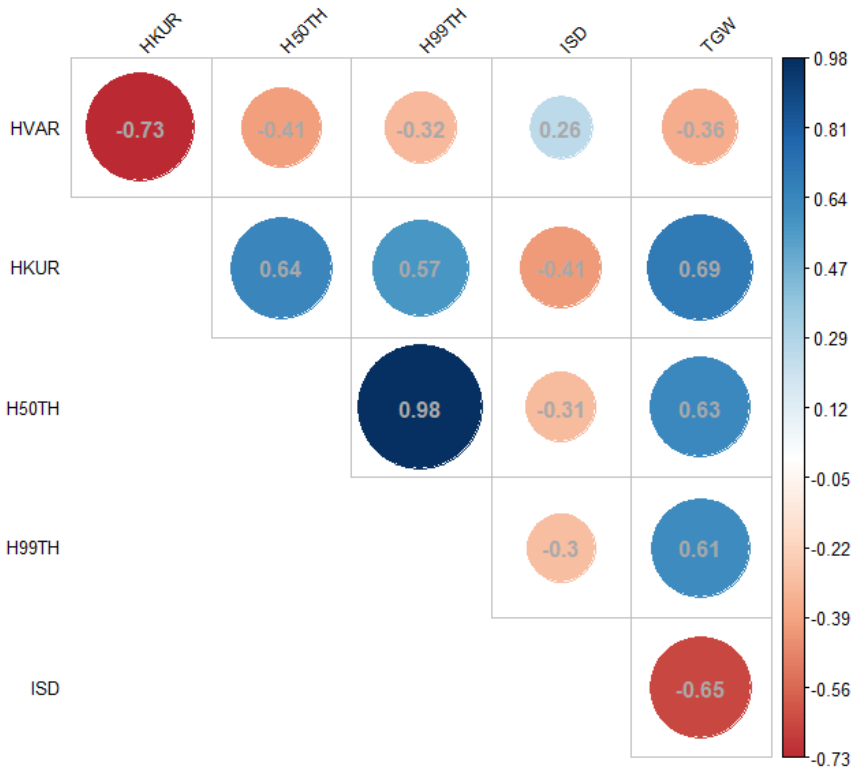

Figure 3. 4 Pearson correlation matrix of variables selected and dependent variable, green weight estimated from field measurements.

Table 3. 6 Variables selected in the GWOB regression model, along with their corresponding coefficients

Variable	*Coefficient*
(Intercept)	201.71
HVAR	15.56
HKUR	30.85
H50TH	14.77
H99TH	6.90
ISD	-21.62
ICV	19.02
IKUR	-22.27

The table above presents a comprehensive overview of the coefficients derived from the Lasso regression model, which delves into the intricate relationships between PMRC 2016 GWOB tons per acre and UAV LiDAR metrics. Each coefficient is intricately linked to a specific UAV LiDAR metric and serves as an estimate of the metric's influence on GWOB. For instance, the coefficient of 15.56 for HVAR illuminates a positive association between the variance of height and GWOB which means an increase in HVAR results in an increase in green weight estimates. Conversely, the coefficient of -21.62 for ISD denotes a negative correlation, signifying that greater values of the standard deviation in intensity metric correspond to decreased GWOB.

Table 3. 7 Adjusted R^2, RMSE (Root Mean Square Error), Mean Bias Error (Bias), and AIC (Akaike Information Criterion) values for both the LASSO GWOB best model and the cross-validation model.

RMSE (tons/acre)		**Adj. R2**		**Bias (tons/acre)**		**AIC**
Best_model	CV	Best_model	CV	Best_model	CV	-292317
33.90	36.62	0.79	0.77	-2.72E-15	1.82E-14	

The findings related to the best model concerning Green Weight Over Bark (GWOB) show an adjusted Adj. R^2 value of 0.79 (n=68), representing a significant proportion, approximately 79%, of the variance in PMRC 2016 total weight tons per acre. Furthermore, the Root Mean Square Error (RMSE), of 33.90 tons/acre, with negligible mean bias error. During cross-validation, the model upholds its performance, giving an Adj. R^2 value of 0.77 and an RMSE of 36.62 tons/acre, while continuing to exhibit minimal bias. Furthermore, the Akaike Information Criterion (AIC) provides additional validation, affirming the model's ability to explain the underlying data while holding to the principle of parsimony.

Figure 3.5 shows the predicted versus actual green weight from the model. The abline and regression lines are almost on top of each other signifies that model predicted values very well. Also, the residual plot and histogram, both presented in the figure, offer supplementary insights by highlighting the absence of any shapes in residual plot and bell-shaped histogram showing the model's effectiveness in summarizing the inherent variability within the dataset.

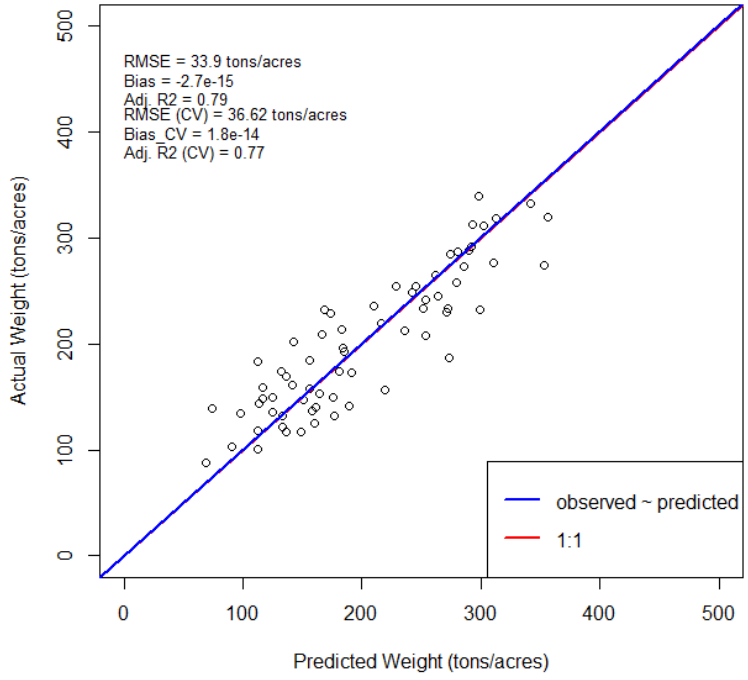

Figure 3. 5 Scatter plot depicting the comparison between predicted and actual green weight (tons per acre) obtained from the best model. The red line is the 1:1 line, and the blue line represents the regression line between observed green weight and predicted green weight from the model.

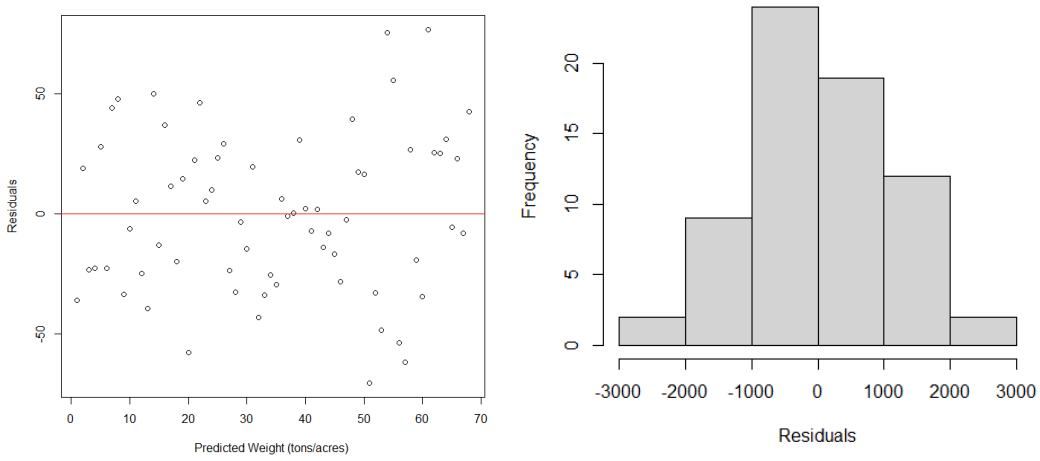

Figure 3. 6 On the left side, the comparison between residual and predicted values for the GWOB model, while on the right side, there is a histogram illustrating the distribution of residuals.

5. DISCUSSION AND CONCLUSION:

Remote sensing data, especially LiDAR acquired through Unmanned Aerial Vehicles (UAV), have emerged as powerful tools in forest inventory and growth modeling. This study focused on the utilization of high point density UAV LiDAR data to model the volume and green weight of the PMRC 2016, specifically within a mature loblolly pine plantation aged between 25-27 years. This research aimed to explore the potential of UAV LiDAR for precise regression modeling using LiDAR-derived metrics. One of the key advantages of using UAV LiDAR is its cost-effectiveness and measurement flexibility. It serves as a valuable alternative to traditional platforms such as aircraft and satellite, which typically offer lower point densities. As studies suggested that the UAV LiDAR sensor higher point density allows for more detailed and accurate data collection (Torresan et al., 2017). Green et al. (2020b) has investigated the use of lower resolution elevation models and less dense LiDAR point clouds for volume estimation in loblolly plantations. They suggested that sparse point clouds could improve the precision of inventory estimates. However, studies mainly considered ALS or natural forests, and the application of point cloud densities in planted forests using UAV LiDAR data with high point density has received limited attention in the literature (Næsset, 2009; Wallace et al., 2012).

The current study aimed to bridge this gap by examining the correlation between UAV 3D point cloud metrics with increased resolution and the volume and green weight using PMRC 2016 equations. The results indicate that UAV-derived metrics can successfully model these forest attributes. As Garcia et al. (2017) emphasized that distributional metrics of LiDAR are closely linked to the return point cloud of data, the high-resolution data used in this study likely contributed to the accuracy of these metrics. The high adjusted R^2 value, coupled with lower Root Mean Square

Error (RMSE) and Bias from both models, suggests that UAV LiDAR can provide detailed and reliable information at the plot level, which can subsequently be upscaled to the operational level for forest inventory purposes.

In conclusion, this study demonstrated the potential of UAV LiDAR data with high point density for accurately modeling the volume and green weight of a mature loblolly pine plantation. The distributional metrics derived from the LiDAR point cloud data played a crucial role in achieving robust results. The high adjusted R^2 values, along with reduced RMSE and Bias, support the use of UAV LiDAR as an effective tool for obtaining detailed forest inventory information at the plot level. To further enhance the effectiveness of such models, it is recommended that future studies consider incorporating individual tree locations. This approach would enable exact estimates of individual trees, facilitating more robust comparisons and enhancing the precision of forest attribute estimates. Consequently, it is advisable to explore this avenue in future research to refine the accuracy of forest inventory assessments using UAV LiDAR technology.

6. REFRENCES:

- Adhikari, A., Montes, C. R., & Peduzzi, A. (2023). A Comparison of Modeling Methods for Predicting Forest Attributes Using Lidar Metrics. *Remote Sensing*, *15*(5). https://doi.org/10.3390/rs15051284
- Arabatzis, A. A., & Burkhart, H. E. (1992). An evaluation of sampling methods and model forms for estimating height-diameter relationships in loblolly pine plantations. *Forest science*, *38*(1), 192-198.
- Avery, T. E., & Burkhart, H. E. (2015). *Forest Measurements*. Waveland Press, Incorporated. https://books.google.com/books?id=_T1ArgEACAAJ
- Borders, B., Zhao, D., Wang, M., & Kane, M. (2014). Growth and yield models for second/third rotation loblolly pine plantations in the Piedmont/Upper Coastal Plain and Lower Coastal Plain of the southeastern US. *University of Georgia, PMRC Technical Report*, *1*, 49.
- Buford, M. A., & Burkhart, H. E. (1987). Genetic improvement effects on growth and yield of loblolly pine plantations. *Forest science*, *33*(3), 707-724.
- Edson, C., & Wing, M. G. (2011). Airborne Light Detection and Ranging (LiDAR) for Individual Tree Stem Location, Height, and Biomass Measurements. *Remote Sensing*, *3*(11), 2494-2528. https://doi.org/10.3390/rs3112494
- Garcia, M., Saatchi, S., Ferraz, A., Silva, C. A., Ustin, S., Koltunov, A., & Balzter, H. (2017). Impact of data model and point density on aboveground forest biomass estimation from airborne LiDAR. *Carbon balance and management*, *12*(1), 1-18.
- Green, P. C., Burkhart, H. E., Coulston, J. W., Radtke, P. J., & Thomas, V. A. (2020). Auxiliary information resolution effects on small area estimation in plantation forest inventory. *Forestry: An International Journal of Forest Research*, *93*(5), 685-693. https://doi.org/10.1093/forestry/cpaa012
- Hyyppä, J., Hyyppä, H., Yu, X., Kaartinen, H., Kukko, A., & Holopainen, M. (2017). Forest inventory using small-footprint airborne LiDAR. In *Topographic laser ranging and scanning* (pp. 335-370). CRC Press.
- Maltamo, M., Eerikäinen, K., Pitkänen, J., Hyyppä, J., & Vehmas, M. (2004). Estimation of timber volume and stem density based on scanning laser altimetry and expected tree size distribution functions [Article]. *Remote Sensing of Environment*, *90*(3), 319-330. https://doi.org/10.1016/j.rse.2004.01.006
- McKeand, S. E. (2019). The Evolution of a Seedling Market for Genetically Improved Loblolly Pine in the Southern United States. *Journal of Forestry*, *117*(3), 293-301. https://doi.org/10.1093/jofore/fvz006
- Miller, J. H., Zutter, B. R., Zedaker, S. M., Edwards, M. B., Haywood, J. D., & Newbold, R. A. (1991). A regional study on the influence of woody and herbaceous competition on early loblolly pine growth. *Southern Journal of Applied Forestry*, *15*(4), 169-179.
- Næsset, E. (1997b). Estimating timber volume of forest stands using airborne laser scanner data. *Remote Sensing of Environment*, *61*(2), Pages 246-253. https://doi.org/https://doi.org/10.1016/S0034-4257(97)00041-2
- Næsset, E. (2009). Effects of different sensors, flying altitudes, and pulse repetition frequencies on forest canopy metrics and biophysical stand properties derived from

small-footprint airborne laser data. *Remote Sensing of Environment*, *113*(1), 148-159. https://doi.org/10.1016/j.rse.2008.09.001

- Nelson, R., Krabill, W., & MacLean, G. (1984). Determining forest canopy characteristics using airborne laser data. *Remote Sensing of Environment*, *15*(3), 201-212.
- Nelson, R., Oderwald, R., & Gregoire, T. G. (1997). Separating the ground and airborne laser sampling phases to estimate tropical forest basal area, volume, and biomass. *Remote Sensing of Environment*, *60*(3), 311-326.
- Nilsson, M. (1996). Estimation of tree heights and stand volume using an airborne lidar system. *Remote Sensing of Environment*, *56*(1), 1-7.
- Pienaar, L., & Shiver, B. (1993). Early results from an old-field loblolly pine spacing study in the Georgia Piedmont with competition control. *Southern Journal of Applied Forestry*, *17*(4), 193-196.
- Ross Nelson, W. K., John Tonelli. (1988). Estimating Forest Biomass and Volume Using Airborne Laser Data. *Remote Sensing of Environment*, *24*(2), 247-267. https://doi.org/https://doi.org/10.1016/0034-4257(88)90028-4
- Rothmund, S., Vouillamoz, N., & Joswig, M. (2017). Mapping slow-moving alpine landslides by UAV—Opportunities and limitations. *The Leading Edge*, *36*(7), 571-579.
- Sayer, M. S., Goelz, J., Chambers, J., Tang, Z., Dean, T., Haywood, J., & Leduc, D. (2004). Long-term trends in loblolly pine productivity and stand characteristics in response to thinning and fertilization in the West Gulf region. *Forest Ecology and Management*, *192*(1), 71-96.
- Sumnall, M. J., Albaugh, T. J., Carter, D. R., Cook, R. L., Hession, W. C., Campoe, O. C., Rubilar, R. A., Wynne, R. H., & Thomas, V. A. (2022). Effect of varied unmanned aerial vehicle laser scanning pulse density on accurately quantifying forest structure. *International Journal of Remote Sensing*, *43*(2), 721-750. https://doi.org/10.1080/01431161.2021.2023229
- Thompson, M. T. (1998). *Forest statistics for Georgia, 1997* (Vol. 36). US Department of Agriculture, Forest Service, Southern Research Station.
- Torresan, C., Berton, A., Carotenuto, F., Di Gennaro, S. F., Gioli, B., Matese, A., Miglietta, F., Vagnoli, C., Zaldei, A., & Wallace, L. (2017). Forestry applications of UAVs in Europe: A review. *International Journal of Remote Sensing*, *38*(8-10), 2427-2447.
- Wallace, L., Lucieer, A., Watson, C., & Turner, D. (2012). Development of a UAV-LiDAR System with Application to Forest Inventory. *Remote Sensing*, *4*(6), 1519-1543. https://doi.org/10.3390/rs4061519
- Zhao, K., Suarez, J. C., Garcia, M., Hu, T., Wang, C., & Londo, A. (2018). Utility of multitemporal lidar for forest and carbon monitoring: Tree growth, biomass dynamics, and carbon flux [Article]. *Remote Sensing of Environment*, *204*, 883-897. https://doi.org/10.1016/j.rse.2017.09.007
- Zolkos, S. G., Goetz, S. J., & Dubayah, R. (2013). A meta-analysis of terrestrial aboveground biomass estimation using lidar remote sensing. *Remote Sensing of Environment*, *128*, 289-298. https://doi.org/10.1016/j.rse.2012.10.017

CONCLUSION:

In summary, this thesis has presented an effective LiDAR-derived tree height estimation method based on the pixel_metrics approach, offering a compelling alternative with reduced instrumental errors and the elimination of operator-based errors in the context of forest growth and yield models. It has successfully addressed the issue of dominant height definition, which tends to overlook the variability of trees across a plot, consequently leading to overestimations in dominant height for modeling purposes.

The pixel_metrics method, by generating a raster of the highest laser points within a plot, accommodates this variability and offers a more comprehensive representation of the forest ecosystem. Furthermore, this study conducted an extensive evaluation of the performance of projected tree heights within projection models and, subsequently, yield predictions. The results demonstrated that the utilization of LiDAR-derived height data slightly enhanced the accuracy of volume and green weight predictions for the second year.

However, it is essential to acknowledge the study's limitations, as it relied on field-measured heights as the reference point for comparison due to the absence of destructive sampling. Actual comparison with destructive data may yield different results. This opens avenues for future research to conduct comprehensive studies comparing LiDAR-derived pixel_metrics heights in height projection models and their implications for growth and yield projections. Such investigations promise to enhance our understanding of the potential of LiDAR technology in forest management and its contributions to more accurate predictive models.

REFRENCES:

- Avery, T. E., & Burkhart, H. E. (1983). *Forest measurements* (3rd ed.) [Bibliographies
- Non-fiction]. McGraw-Hill. https://search.ebscohost.com/login.aspx?direct=true&AuthType=ip,shib&db=cat06564a&AN=uga.997790773902959&site=eds-live&custid=uga1
- Bortolot, Z. J., & Wynne, R. H. (2005). Estimating forest biomass using small footprint LiDAR data: An individual tree-based approach that incorporates training data. *ISPRS Journal of Photogrammetry and Remote Sensing*, *59*(6), 342-360. https://doi.org/10.1016/j.isprsjprs.2005.07.001
- Cao, L., Coops, N. C., Innes, J. L., Sheppard, S. R. J., Fu, L., Ruan, H., & She, G. (2016). Estimation of forest biomass dynamics in subtropical forests using multi-temporal airborne LiDAR data. *Remote Sensing of Environment*, *178*, 158-171. https://doi.org/10.1016/j.rse.2016.03.012
- Harrison, W. M., & Borders, B. E. (1996). Yield prediction and growth projection for site-prepared loblolly pine plantations in the Carolinas, Georgia, Alabama, and Florida. https://doi.org/http://pmrc.uga.edu/TR1996-1.pdf
- Hopkinson, C., Chasmer, L., & Hall, R. J. (2008). The uncertainty in conifer plantation growth prediction from multi-temporal lidar datasets. *Remote Sensing of Environment*, *112*(3), 1168-1180. https://doi.org/10.1016/j.rse.2007.07.020
- Hudak, A. T., Evans, J. S., & Stuart Smith, A. M. (2009). LiDAR utility for natural resource managers. *Remote Sensing*, *1*(4), 934-951.
- Jeffrey P. Prestemon, R. C. A. (2002). *Timber products supply and demand. In: Wear, D.N.; Greis, J.G., eds.*
- Matti Maltamo, E. N., Jari Vauhkonen. (2014). *Forestry applications of airborne laser scanning: Concepts and case studies*. Springer Dordrecht. https://doi.org/https://doi.org/10.1007/978-94-017-8663-8
- Naesset, E. (1997). Determination of mean tree height of forest stands using airborne laser scanner data. *52*(2), 49-56. https://search.ebscohost.com/login.aspx?direct=true&AuthType=ip,shib&db=edsbl&AN=RN024544941&site=eds-live&custid=uga1
- Popescu, S. C. (2007). Estimating biomass of individual pine trees using airborne lidar. *Biomass and Bioenergy*, *31*(9), 646-655. https://doi.org/10.1016/j.biombioe.2007.06.022
- Schumacher, F. X., & Hall, F. d. S. (1933). Logarithmic expression of timber-tree volume.
- Silva, C. A., Klauberg, C., Hudak, A. T., Vierling, L. A., Jaafar, W. S. W. M., Mohan, M., Garcia, M., Ferraz, A., Cardil, A., & Saatchi, S. (2017). Predicting stem total and assortment volumes in an industrial Pinus taeda L. forest plantation using airborne laser scanning data and random forest [Journal Article]. *Forests*, *8*(7), 254. https://doi.org/10.3390/f8070254
- https://www.mdpi.com/1999-4907/8/7/254/htm

- Yang, S.-I., & Burkhart, H. E. (2020). Evaluation of total tree height subsampling strategies for estimating volume in loblolly pine plantations. *Forest Ecology and Management*, *461*. https://doi.org/10.1016/j.foreco.2020.117878